REPORT No. 188 S
(S 2/155)

August 1974

NEDERLANDS SCHEEPSSTUDIECENTRUM TNO
NETHERLANDS SHIP RESEARCH CENTRE TNO
SHIPBUILDING DEPARTMENT LEEGHWATERSTRAAT 5, DELFT

★

THE BEHAVIOUR OF A SHIP IN HEAD WAVES AT RESTRICTED WATER DEPTHS

(HET GEDRAG VAN EEN SCHIP IN KOPGOLVEN BIJ BEPERKTE WATERDIEPTEN)

by

DR. IR. J. P. HOOFT
(Netherlands Ship Model Basin)

Issued by the Council

VOORWOORD

Voor de huidige grote en zeer grote schepen zijn bepaalde zeeën in belangrijke vaarroutes niet meer als diep te beschouwen, zoals bijvoorbeeld grote gedeelten van de Noordzee. Aangezien in deze gebieden een behoorlijke golfslag kan optreden bestaat de mogelijkheid dat het schip als gevolg van haar bewegingen de zeebodem raakt. Het is daarom van belang om ook inzicht te hebben in de grootte van de mogelijk optredende scheepsbewegingen in golven op niet meer diep water, waarvan, in tegenstelling tot de gedragingen op diep en ondiep water, nog weinig bekend is.

Het gevaar van het raken van de zeebodem wordt bepaald door de bewegingen in het langsscheepse vlak, zodat squat en trim van het schip in vlak water moet worden beschouwd tesamen met stampen en dompen in golven.

Voor dit onderzoek zijn reeds eerder modelproeven uitgevoerd in voor inkomende golven bij een drietal verhoudingen van de diepgang tot de waterdiepte.

Naast de modelproeven zijn theoretische berekeningen uitgevoerd om voorspellingen te kunnen doen van de optredende squat en trim in vlak water. De stamp en domp bewegingen voor ondiep water zijn berekend door uit te gaan van de bewegingsvergelijkingen voor diep water.

Voor de scheepsvorm is gebruik gemaakt van een model, behorende tot de series „60" met $CB = 0.80$, waarvan het gedrag in diep water uitgebreid is onderzocht.

De voor dit onderzoek gehouden modelproeven en de berekeningen zijn alle uitgevoerd bij het Nederlandsch Scheepsbouwkundig Proefstation te Wageningen.

HET NEDERLANDS SCHEEPSSTUDIECENTRUM TNO

PREFACE

Several seas in the important trade routes can no longer be considered as deep with respect to the large and giant ships of this time. This holds for example for large parts of the North Sea too. As considerable seas can appear in these areas it is possible that the ship hits the bottom because of her motions. It is therefore important to have insight into the values of the ship motions that can be experienced in waves at waters of restricted depth too, of which, contrary to the behaviour at deep and shallow water, still little is known.

The danger of bottom contact depends upon the motions in the longitudinal plane, because of which squat and trim of the ship in calm water has to be considered in combination with heave and pitch in waves.

Model experiments have been executed earlier in head waves at three values of the depth to draught ratio. In addition to the model experiments theoretical calculations have been made to predict the squat and trim. The pitch and heave motions at restricted water have been calculated starting from the equations of motion for deep water.

The ship form was based upon a model of the "series 60" ships with $CB = 0.80$, of which the behaviour in deep water was determined extensively in previous research.

The model experiments and calculations made for this project were executed at the Netherlands Ship Model Basin, at Wageningen.

THE NETHERLANDS SHIP RESEARCH CENTRE TNO

CONTENTS

LIST OF SYMBOLS

a_{ij}	Added mass in the i-direction due to a motion in the j-direction
b_{ij}	Damping coefficient in the i-direction due to a motion in the j-direction
c_{ij}	Spring constant in the i-direction due to a motion in the j-direction
c	Some coefficient
d	water depth
e	2.72
f	Some coefficient
g	Acceleration due to gravity
i	$\sqrt{-1}$
m	Mass of body
t	Time
V	Forward speed
x	Longitudinal motion
y	Lateral motion
z	Vertical motion
A_i, B_i	Response functions of motion in i-direction due to a unit vertical force (A) and pitching moment (B)
B	Breadth of ship
F_n	Froude number
I_{ii}	Moment of inertia of body about axis in i-direction
L_{pp}	Length between perpendiculars
M	Wave excited pitching moment
T	Draught of ship
V_{mn}	$(\delta_{mn}m_m + a_{mn})(i\omega)^2 + b_{mn}(i\omega) + c_{mn}$
W_{mn}	$(\delta_{mn}m_m + a_{mn})\,d^2/dt^2 + b_{mn}d/dt + c_{mn}$
Z	Wave excited vertical force
$\varepsilon_{i\zeta}$	Phase difference between wave motion and ship motion in i-direction
$\sigma_{i\zeta}$	Phase difference between wave motion and wave excited force in i-direction
ω	Wave circular frequency
ω_e	Circular frequency of wave encounter = circular frequency of oscillation of ship
ζ	Wave motion
θ	Pitch angle
κ	Wave number $= 2\pi/\lambda$
λ	Wave length
μ	Wave direction relative to ship direction (positive when turning counter-clockwise)
μ	Some coefficient
δ_{mn}	1 when $m = n$ 0 when $m \neq n$

THE BEHAVIOUR OF A SHIP IN HEAD WAVES AT RESTRICTED WATER DEPTHS

by

Dr. Ir. J. P. HOOFT

Summary

In this paper results will be presented of tests with models sailing in head waves at restricted water depths of 1.875, 2.5 and 3.75 times the ship's draught. Also results will be given of calculated ship motions in deep water. No attention will be paid to ship motions in shallow water.

A discussion will be given about the influences of the water depth on the ship motions. It will be shown how the ship motions at restricted water depths can be determined from the ship motions in deep water.

1 Introduction

From a point of view of ship motions, three areas can be distinguished in which large ships sail.

a. Deep water (infinite depth: water depth > 4 times the draught) where a ship sails at a service speed which can be influenced by the condition of the sea.
b. Water with restricted or finite depth (4 times the draught > water depth > approx. 2 times the draught), where a ship still sails at as large a speed as possible, during which an influence of the sea bottom can be noticed.
c. Shallow water (water depth < approx. 2 times the draught), where the ship speed has to be decreased to avoid bottom contact due to the ship's velocity or due to the ship's motions as influenced by shallow water waves.

With respect to the ship motions in the first and third area extensive research has already been performed (see [1], [2], [3]). For the second area, however, little is known. For this reason an investigation has been performed to determine the behaviour of a ship in waters with finite depth. The results of this investigation are given in the present paper.

When sailing in areas with restricted water depth, the following will occur.

1. The squat and trim will change in comparison to the values at deep water.
2. The ship motions will change in comparison to the motions at deep water.
3. The external loadings on the ship will change in comparison with the loadings at deep water.

In order to determine these changes tests have been carried out with a model of the "series 60" with a block coefficient of 0.80. The results of these tests have been compared with the results of theoretical investigations.

The model tests have been carried out in the shallow water basin of the Netherlands Ship Model Basin at three water depths (1.875, 2.500, 3.750 × draught) in still water and in regular head waves. The width of the basin amounts to 15.75 m being about 25 times the ship's breadth.

2 Description of ship model

The dimensions of the wooden model are given in Table I. A body plan with the outlines of the bow and the stern is shown in figure 1. The model was fitted with a stock propeller according to figure 2 and Table II, a rudder and bilge keels. The bow of the model was provided with a row of studs to stimulate a turbulent flow about the hull.

Table I. Particulars of model

designation	symbol	unit	model 2940[z]
Length between perpendiculars	L_{pp}	m	4.289
Length on waterline	L_{wl}	m	4.360
Breadth moulded	B	m	0.613
Draft moulded (even keel)	T	m	0.245
Displacement volume moulded		m^3	0.5152
Longitudinal centre of buoyancy abaft of *FP*	$\overline{FB}$	m	2.037
Block coefficient	C_B		0.800
Midship section coefficient	C_M		0.994
Prismatic coefficient	C_P		0.805
Designed load waterline coefficient	C_{wl}		0.871
Centre of gravity above keel	$\overline{KG}$	m	0.218
Metacentric height	$\overline{GM}$	m	0.0307
Longitudinal radius of gyration for pitching	K	m	1.030 ($=0.24\times L_{pp}$)

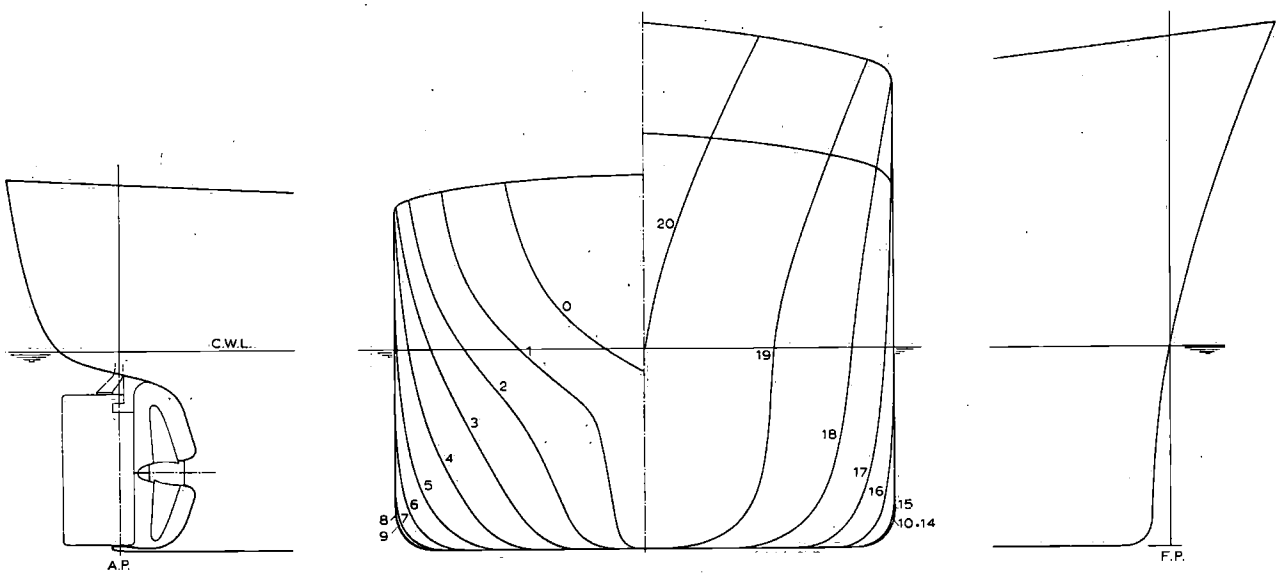

Fig. 1. Body plan with bow and stern outlines of tested "series 60" model.

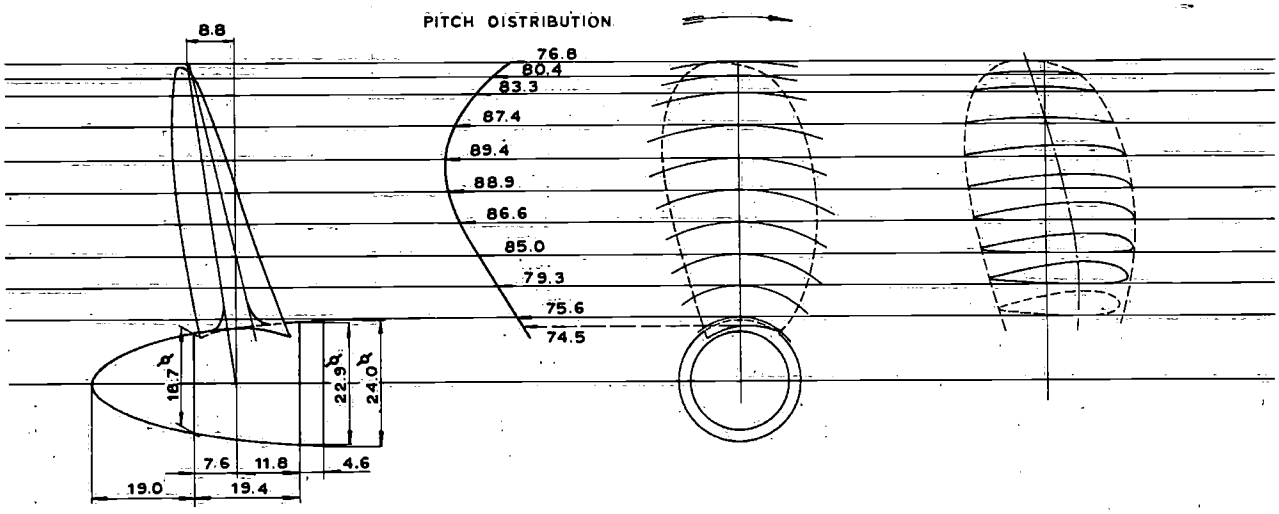

Fig. 2. Propeller model used during self-propulsion tests in still water and waves.

Table II. Propeller data

designation	symbol	unit	model
Diameter	D	mm	119.00
Pitch at blade tip		mm	76.80
Pitch at 0.7 radius	$P_{0.7R}$	mm	89.40
Pitch at root		mm	74.50
Pitch ratio	$P_{0.7R}/D$		0.751
Boss-Diameter ratio	d/D		0.173
Expanded blade area ratio	A_E/A_O		0.463
Number of blades	Z		4

3 Squat and trim of ship in still water

The squat of a ship is defined as the mean sinkage of the centre of gravity due to the forward speed. The trim is defined as the mean change of longitudinal inclination of the ship with respect to the inclination at zero speed. As a result of the passing ship, the fluid particles in the vicinity of the ship's hull are accelerated from zero to a certain velocity, which induces, according to Bernoulli, a decrease of the pressure resulting in a downward displacement of the vessel. It will be clear that the distribution of the pressure over the length of the ship generally induces a change of trim of the vessel as well.

As the propeller induces an additional velocity field in the vicinity of the aft part of the ship, the mean sinkage and trim will also be affected by the propulsion system. A reduction of the underkeel clearance will constrict the effective channel of flow (blockage effect) resulting in a greater velocity of the water particles underneath the ship which leads to an increase of sinkage.

During the squat tests in still water the vertical

motions at the fore and aft perpendicular were measured with respect to a carriage running above the self-propelled model. The number of revolutions of the propeller required to propel the model at the desired speed, was kept constant during a test run.

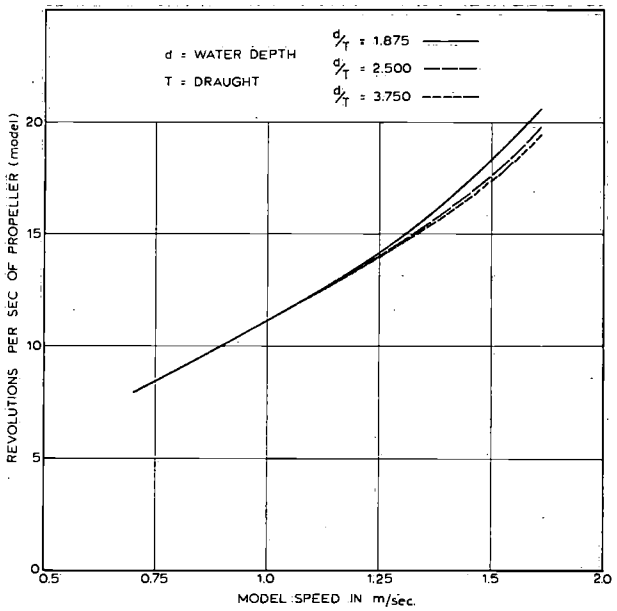

Fig. 3. Relationship between model speed and propeller RPM for several d/T ratios.

The RPM – speed relationship for the various water depths is given in figure 3. The model was accelerated by the carriage and released after the required speed had been reached. During all tests the model was kept on a straight course by means of a "trimming" device which allows the model to move freely in the vertical plane see figure 4.

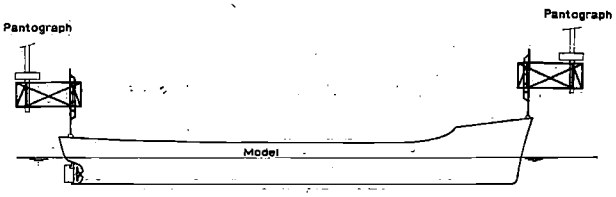

Fig. 4. Test set-up for squat measurements.

The results of the model tests confirm (especially for shallower water) the results of the study by Tuck and Taylor [4] as can be seen from figures 5 and 6 in which the model test results are plotted in comparison with the calculations, the equations given by Tuck being used.

Tuck and Taylor deal with the problem of a ship sailing in an infinite expanse of water in a two-dimensional way. The velocity potential for the flow around the ship is derived from which the pressure

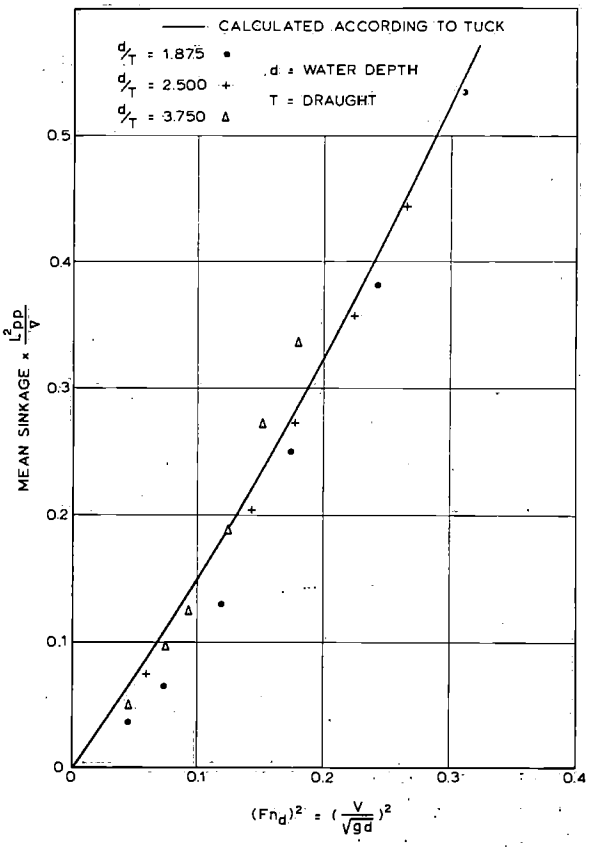

Fig. 5. Measured and calculated mean sinkage (squat).

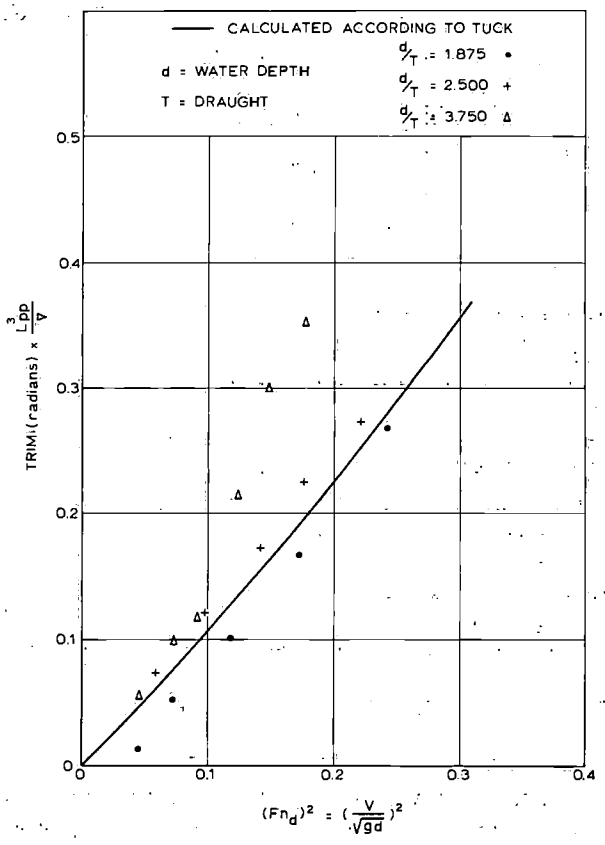

Fig. 6. Measured and calculated trim.

decrease is determined. Integration of the vertical component of the pressure over the ship's hull leads to the change of upward force which can easily be translated into a change of sinkage. The same holds true for the trimming moment and consequently the change of trim.

From the investigations by Tuck the following equations are obtained:

The squat (mean sinkage of centre of gravity) can be written as

$$\bar{z}_{\text{mean}} = \frac{F_n^2(d)}{\sqrt{1-F_n^2(d)}} \cdot c_z \cdot \frac{\nabla}{L_{pp}^2} \tag{1}$$

while (assuming that $\overline{M_L G} = \overline{M_L B}$) the change of trim satisfies

$$\theta = \frac{F_n^2(d)}{\sqrt{1-F_n^2(d)}} \cdot c_\theta \cdot \frac{\nabla}{L_{pp}^3} \tag{2}$$

in which

$F_n(d)$ = Froude number based on the water depth = $v_m/\sqrt{gd}$

v_m = model speed

d = water depth

c_z, c_θ = dimensionless shape factors of ship's hull

$$c_z = \frac{2\pi L_{pp}^2 \int_0^{L_{pp}} dx \int_0^{L_{pp}} d\xi \cdot B'_{(x)} \cdot S'_{(\xi)} \cdot \log(x-\xi)}{A_{wl} \cdot \nabla} \tag{3}$$

$$c_\theta = \frac{2\pi L_{pp}^3 \int_0^{L_{pp}} dx \int_0^{L_{pp}} d\xi (B_{(x)} \cdot x)' \cdot S'_{(\xi)} \cdot \log(x-\xi)}{I_{wl} \cdot \nabla} \tag{4}$$

in which

L_{pp} = length of ship between perpendiculars

$B_{(x)}$ = breadth of ship on waterline at station x

$S_{(x)}$ = area of cross section at station x

A_{wl} = waterline area

I_{wl} = moment of inertia of waterline area

∇ = volume of displacement

$\overline{M_L G}$ = longitudinal metacentric height

$\overline{M_L B}$ = height of longitudinal metacentre M_L above centre of buoyancy

According to Tuck c_z varies between 1.40 and 1.53 over a wide range of ship forms of which the value $c_z = 1.46$ is recommended. When using the value $c_\theta = 1$ for the calculations of the change of trim a good agreement between calculations and model measurements was found (Fig. 6). For a better determination of the c_z and c_θ values from the equations (3) and (4) the approximations given by Vermeer [5] are recommended.

From equations (1) and (2) it can easily be seen that the squat and the trim are proportional to the block coefficient of the ship and inversely proportional to the length/breadth ratio and the water depth/draught ratio. The good agreement between the theory of Tuck and the measurements seems to demonstrate the lack of scale effect in the tests. However, it should be noted that this theory does not take the induced velocities of the propeller into account and assumes no flow separation at the aft body. Tests reported by Stumpf [6] and Bazilevsky [7] show clearly that during resistance tests (no propeller action) separation of the boundary layer occurs.

This separation disappears for the greater part during propulsion tests in the range of low advance ratios J (heavy propeller loads). Diminishing the boundary layer separation will generally increase the pressure at the aft body, but due to the extra velocities induced by the screw, the total pressure decreases considerably which was clearly shown by Bazilevsky.

The good agreement between the mean measured sinkage and the sinkage calculated according to the potential theory will therefore most probably be caused by the prevention of boundary layer separation due to the heavy load of the propeller.

The lack of boundary layer separation was one of the assumptions of the calculations.

4 Equations of motions of ships in waves

For the present study tests have been performed in regular head waves. As a consequence the ship motions can be described as a combination of pitch and heave, which can be written in a general way by

$$\begin{aligned}
&(m+a_{zz})\ddot{z} + b_{zz}\dot{z} + c_{zz}z + a_{z\theta}\ddot{\theta} + b_{z\theta}\dot{\theta} + c_{z\theta}\theta = \\
&= Z_a \cos(\omega_e t + \sigma_z) \\
&(I_{\theta\theta} + a_{\theta\theta})\ddot{\theta} + b_\theta\dot{\theta} + c_{\theta\theta}\theta + a_{\theta z}\ddot{z} + b_{\theta z}\dot{z} + c_{\theta z}z = \\
&= M_a \cos(\omega_e t + \sigma_\theta)
\end{aligned} \tag{5}$$

in which

m = mass of the ship

$I_{\theta\theta}$ = moment of inertia of ship about the transverse axis

$a_{ij} b_{ij}$ = hydrodynamic coefficients of the ship introducing the reaction forces

a_{ij} = added mass coefficient

b_{ij} = damping coefficient

c_{ij} = restoring force coefficient (hydrostatic coefficient)

Z_a = wave excited vertical force

M_a = wave excited pitching moment

ω_e = circular frequency of wave encounter

The circular frequency of the waves is defined by ω. It will be obvious that the ship motion frequencies are equal to the beat frequency of the waves on the moving ship which is defined by the frequency of encounter. Therefore the frequency of the ship motions will be indicated further on by ω_e.

The relationship between the frequency of encounter and the wave frequency follows from

$$\omega_e = \omega - \kappa V \cos\mu \qquad (6)$$

in which

κ = wave number = $2\pi/\lambda$

V = speed of ship

μ = wave direction

The relationship of (6) is represented in fig. 7 for $d/T = \infty$, 3.75, 2.50, 1.875.

In order to analyse the ship motions (see [8]) as a response to the wave action it should be noted that

1. The ship coefficients a_{ij}, b_{ij}, c_{ij} depend on
   - the ship's form
   - the frequency of oscillation of the ship
   - the ship speed
   - the water depth

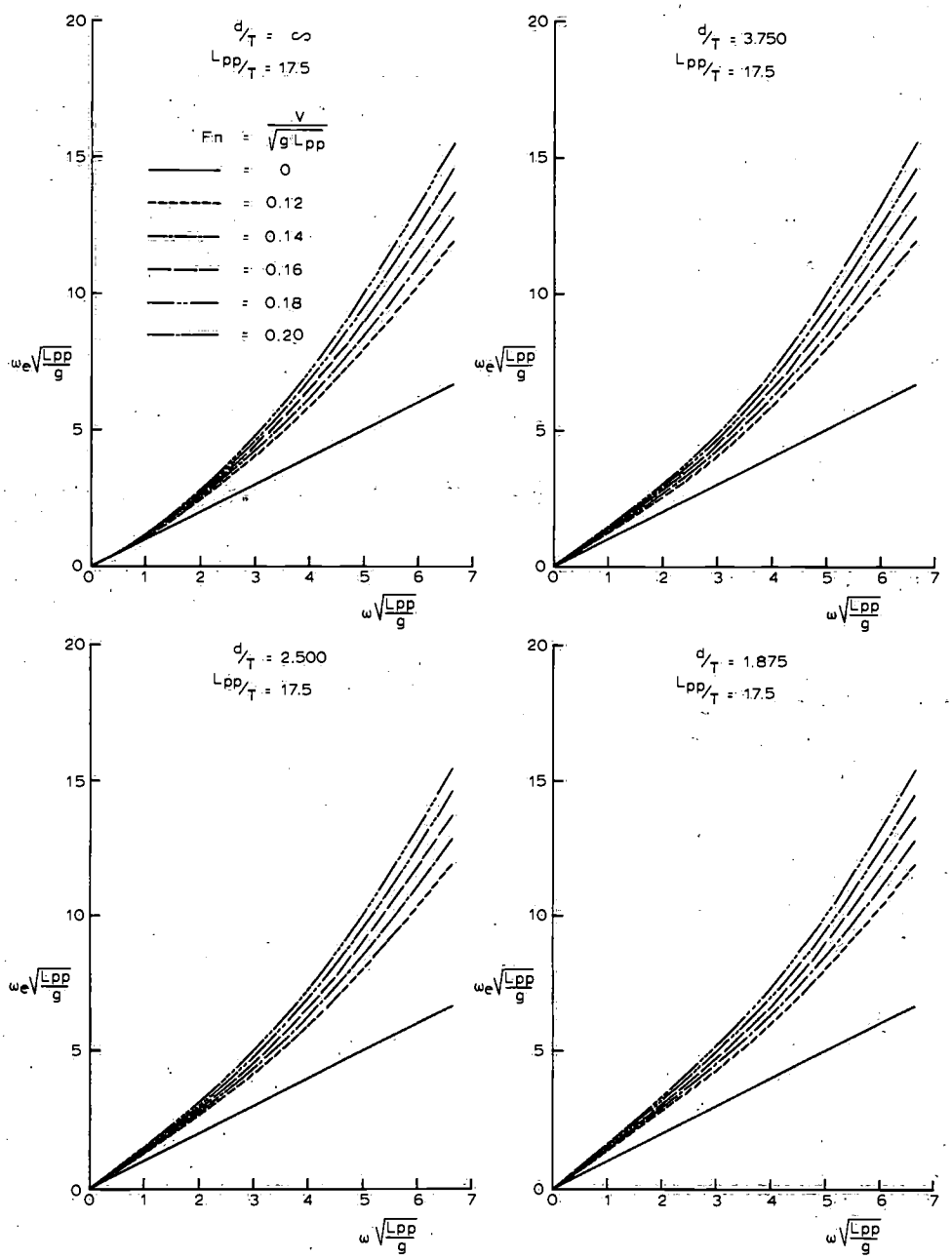

Fig. 7. Relationship between the wave frequency (ω) and frequency of encounter (ω_e) for several ratios of water depth (d) and draught (T); wave direction 180° (head waves).

2. The wave excited forces and moments depend on
   - the ship's form
   - the frequency and height of the waves
   - the ship speed
   - the water depth
   - the wave length relative to the ship length
3. The response operator, being the ratio of motion amplitude to wave amplitude depends on the ratio of frequency of oscillation of the ship to the natural frequency of oscillation of the ship: The natural frequency is defined to be the frequency at which the total reaction force is minimal or in other words the frequency at which the ship motion will be maximal at a given exciting force.

5 Hydrodynamic coefficients of the ship

The influences of the ship speed and the frequency of oscillation on the hydrodynamic coefficients mentioned before were discussed extensively by Vugts [1]. Also the determination of the total hydrodynamic coefficients by integration of the local hydrodynamic coefficients over the ship length is mentioned. At a given cross section of the ship the local hydrodynamic coefficients depend on the form of this cross section.

Instead of analyzing the hydrodynamic coefficients separately the overall effect of the influence of the frequency of oscillation and the ship speed on the reaction of the ship to an exciting force will be elaborated here by means of computer programmes developed at the Netherlands Ship Model Basin by C. Flokstra [10].

Equation (5) can be rewritten as

$$\begin{aligned} W_{zz}z_{(t)} + W_{z\theta}\theta_{(t)} &= Z_{(t)} \\ W_{\theta z}z_{(t)} + W_{\theta\theta}\theta_{(t)} &= M_{(t)} \end{aligned} \tag{6}$$

in which

$$W_{mn} = (\delta_{mn}M_m + a_{mn})\frac{d^2}{dt^2} + b_{mn}\frac{d}{dt} + c_{mn}$$

When the exciting heave force and pitching moment change sinusoidally in time, equation (6) is transformed in

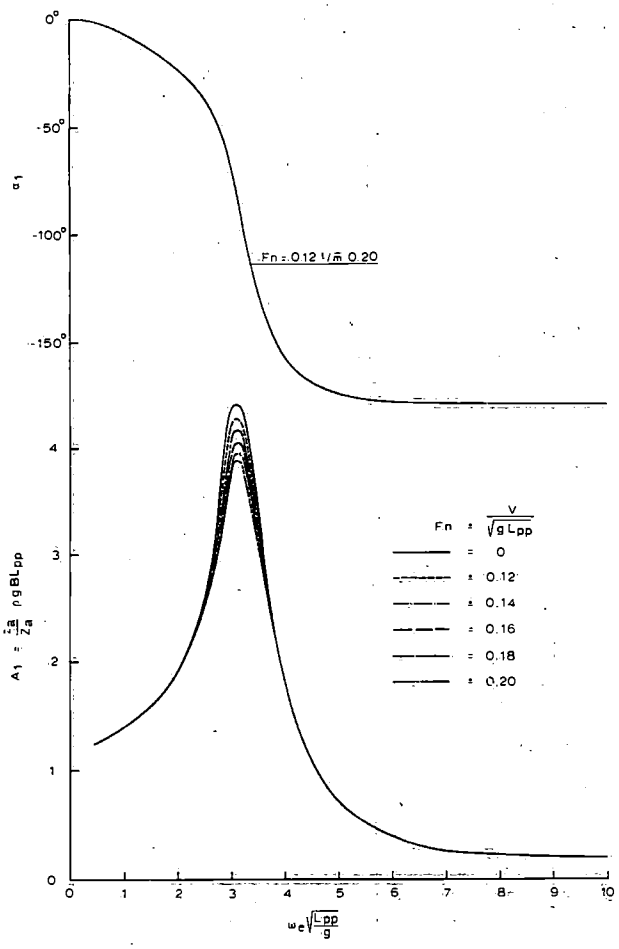

Fig. 8. Uncoupled reaction function $A_1 e^{i\alpha_1}$ of the heave motion $z_a e^{i\varepsilon_z}$ to an oscillating vertical force with amplitude Z_a and frequency ω_e.

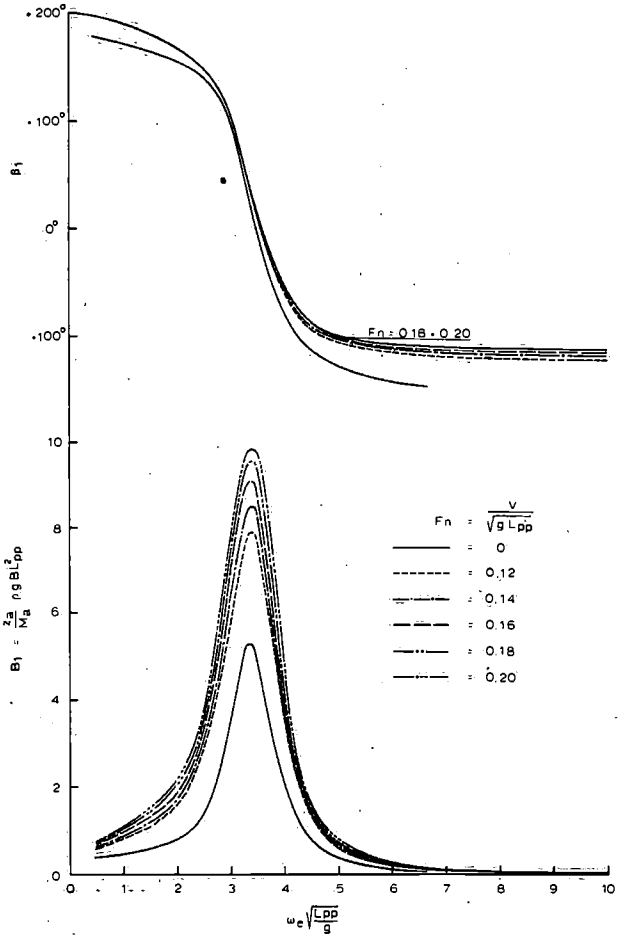

Fig. 9. Coupled reaction function $B_1 e^{i\beta_1}$ of the heave motion $z_a e^{i\varepsilon_z}$ to an oscillating pitching moment with amplitude M_a and frequency ω_e.

$$V_{zz}z_{(\omega)} + V_{z\theta}\theta_{(\omega)} = Z_{(\omega)}$$
$$V_{\theta z}z_{(\omega)} + V_{\theta\theta}\theta_{(\omega)} = M_{(\omega)} \qquad (7)$$

in which

$$V_{mn} = (\delta_{mn}M_m + a_{mn})(i\omega)^2 + b_{mn}(i\omega) + c_{mn}$$

The solution of equation (7) is

$$z_{(\omega)} = \frac{V_{\theta\theta}}{D} Z_{(\omega)} - \frac{V_{z\theta}}{D} M_{(\omega)}$$
$$\theta_{(\omega)} = \frac{V_{zz}}{D} M_{(\omega)} - \frac{V_{\theta z}}{D} Z_{(\omega)} \qquad (8)$$

in which

$$D = V_{zz}V_{\theta\theta} - V_{\theta z}V_{z\theta}$$

From equation (8) the following solution of the heave and pitch response to waves is found

$$\frac{z_a}{\zeta_a} e^{i\varepsilon_z} = A_1 e^{i\alpha_1} \frac{Z_a}{\zeta_a} e^{i\sigma_z} + B_1 e^{i\beta_1} \frac{M_a}{\zeta_a} e^{i\sigma_M}$$
$$\frac{\theta_a}{\zeta_a} e^{i\varepsilon_\theta} = A_2 e^{i\alpha_2} \frac{Z_a}{\zeta_a} e^{i\sigma_z} + B_2 e^{i\beta_2} \frac{M_a}{\zeta_a} e^{i\sigma_M} \qquad (9)$$

in which

z_a = heave amplitude
θ_a = pitch amplitude
ζ_a = wave amplitude
ε_z = phase difference between heave and wave motion
ε_θ = phase difference between pitch and wave motion
Z_a = amplitude of wave excited heave force
M_a = amplitude of wave excited pitch moment
σ_z = phase difference between heave force and wave motion
σ_M = phase difference between pitch moment and wave motion

From figures 8, 9, 10 and 11 the reaction functions $A_1e^{i\alpha_1}$, $B_1e^{i\beta_1}$, $A_2e^{i\alpha_2}$ and $B_2e^{i\beta_2}$ of the ship motions to a unit exciting force or moment as a function of the

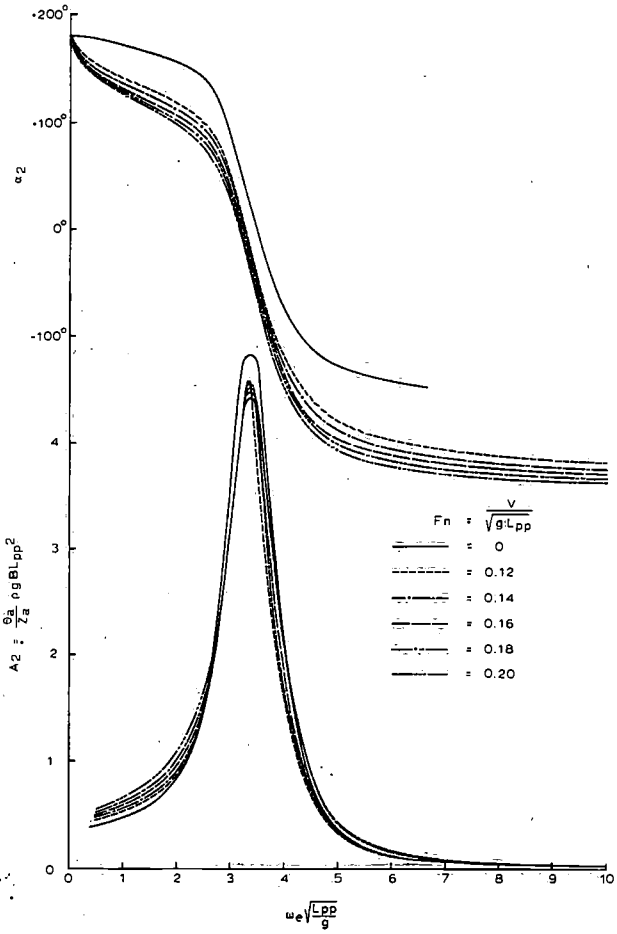

Fig. 10. Coupled reaction function $A_2e^{i\alpha_2}$ of the pitch motion $\theta_a e^{i\varepsilon_\theta}$ to an oscillating vertical force with amplitude Z_a and frequency ω_e.

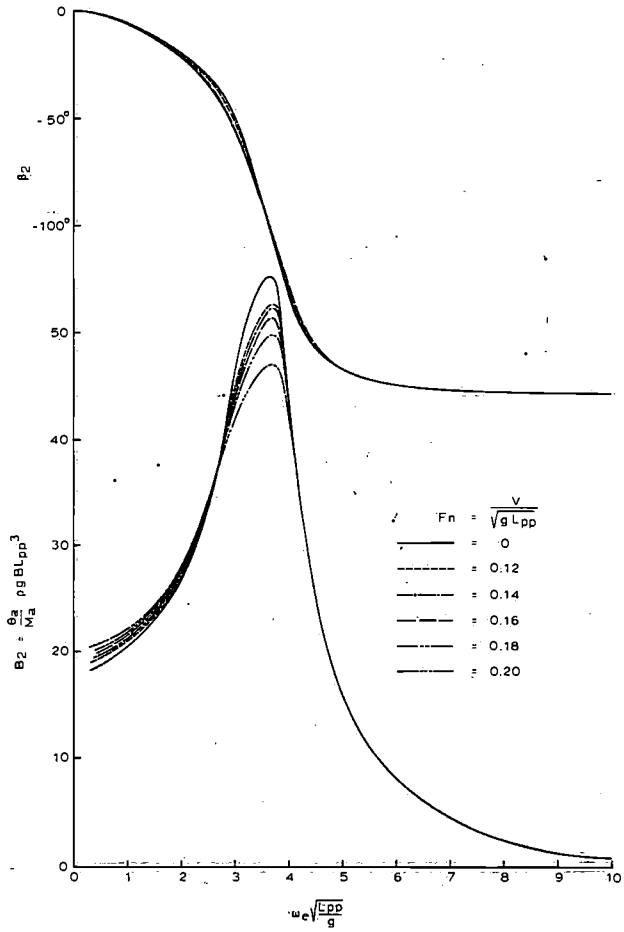

Fig. 11. Uncoupled reaction function $B_2e^{i\beta_2}$ of the pitch motion $\theta_a e^{i\varepsilon_\theta}$ to an oscillating pitching moment with amplitude M_a and frequency ω_e.

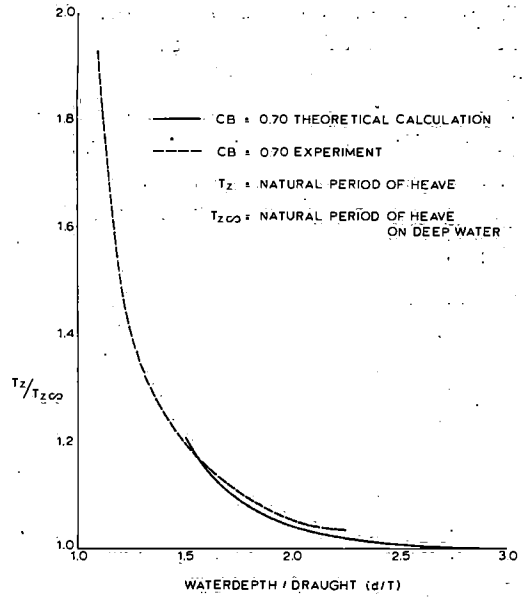

Fig. 12. Influence of water depth on natural period of heave according to Tasai [9].

ship speed and the frequency of oscillation ω_e can be derived.

From these figures the following conclusions can be drawn

1. Except for a frequency range around the natural frequency the uncoupled functions $A_1 e^{i\alpha_1}$ (fig. 8) and $B_2 e^{i\beta_2}$ (fig. 11) are mainly determined by the frequency of oscillation of the ship (frequency of encounter) and are independent of the ship's velocity.
2. The natural frequency is hardly influenced by the ship's velocity.
3. At the natural frequency the reaction functions are influenced by the ship speed. From this it can be seen that the ship speed does influence the damping of the ship.

At changing water depths the hydrodynamic coefficients will change. From ref. [9] the influence of the water depth on the natural heave period has been obtained and plotted in figure 12. From this figure it can be concluded that at water depths larger than

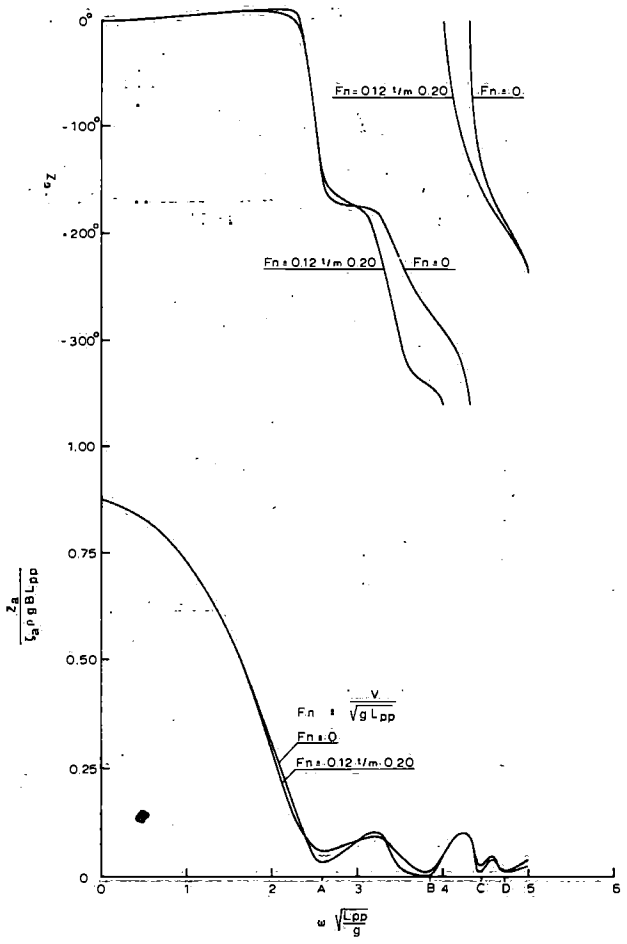

Fig. 13. Influence of ship speed on wave excited vertical force $Z_a e^{i\sigma_Z}$ in deep water; wave direction 180° (head waves).

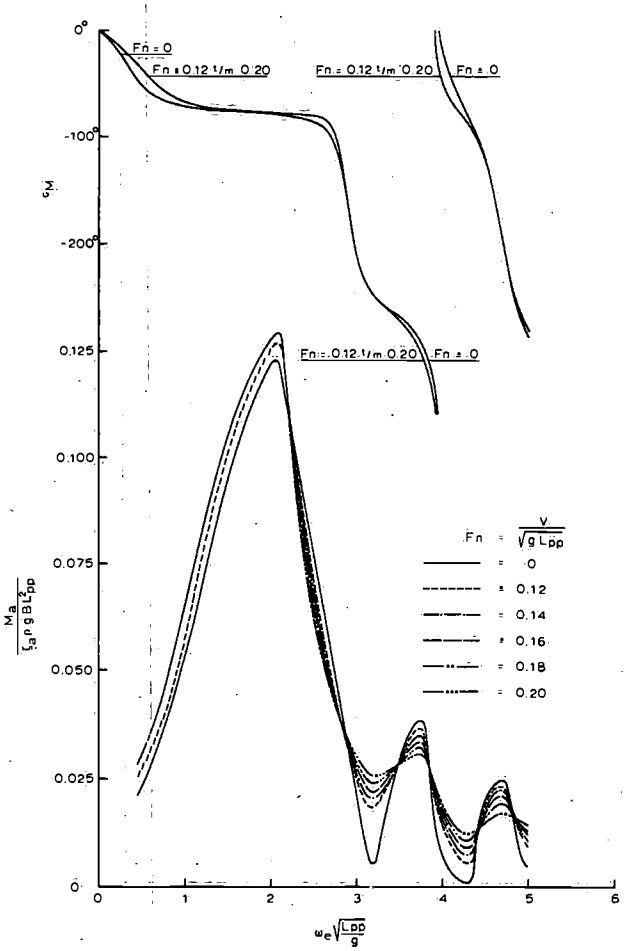

Fig. 14. Influence of ship speed on wave excited pitching moment $M_a e^{i\sigma_M}$ in deep water; wave direction 180° (head waves).

about two times the draught the influence of the water depth on the added mass is negligible.

6 Wave-excited forces on the ship

In order to analyse the influences of the ship speed and the wave frequency on the wave excited forces as mentioned earlier, the wave excited heave force and pitching moment acting on the ship model being studied have been calculated for deep water by means of a computer programme [10].

The results of these calculations are presented in figures 13 and 14.

From these Figures it can be found that the tendencies (locations of maximum and minimum values) of the forces as functions of the wave frequency are not influenced by the ship's velocity which can be explained by the fact that these maximum and minimum values occur at frequencies for which

a. the wave length has a specific value relative to the ship length
b. the inertia forces cancel the Froude-Krilov force.

Both effects are hardly influenced by the ship's velocity. However, the maximum and minimum values of the wave excited force and moment are influenced by the ship speed. Referring to the frequencies mentioned under item a. it will be obvious that for a ship with a constant cross section over the length (l) the total vertical force on the ship can be found from

$$Z = \int_{-\frac{1}{2}l}^{+\frac{1}{2}l} Z'_{(x)}\,dx \tag{10}$$

in which

$Z'_{(x)}$ = wave force per unit length on a cross section of the ship located at a distance x of the centre of the ship
$= Z'_a \sin(\omega t - \kappa x)$

From equation (10) one finds

$$Z = Z'_a \int_{-\frac{1}{2}l}^{+\frac{1}{2}l} \sin(\omega t - \kappa x)\,dx = Z_a \sin \omega t \tag{11}$$

in which

$$Z_a = Z'_a l \frac{\sin \frac{1}{2}\kappa l}{\frac{1}{2}\kappa l} \tag{12}$$

In the same way one finds

$$M_a = Z'_a \cdot \frac{l}{\kappa} \cdot \left\{ \cos(\tfrac{1}{2}\kappa l) - \frac{\sin(\frac{1}{2}\kappa l)}{\frac{1}{2}\kappa l} \right\}$$

From equation (12) it will be clear that the factors

$$f_1 = (\sin \tfrac{1}{2}\kappa l)/\tfrac{1}{2}\kappa l \quad \text{and} \quad f_2 = \frac{1}{\kappa l}\left\{ \cos(\tfrac{1}{2}\kappa l) - \frac{\sin(\frac{1}{2}\kappa l)}{\frac{1}{2}\kappa l} \right\}$$

introduce maximum and minimum values of the wave excited force and moment. In figure 15 and 16 the estimated factors f_1 and f_2 for a ship with a cross section changing over the length of the ship has been plotted for different d/T ratios. For such a ship an equivalent length l has to be taken. In this case for the "series 60" ship $l = 0.85 L_{pp}$ has been chosen.

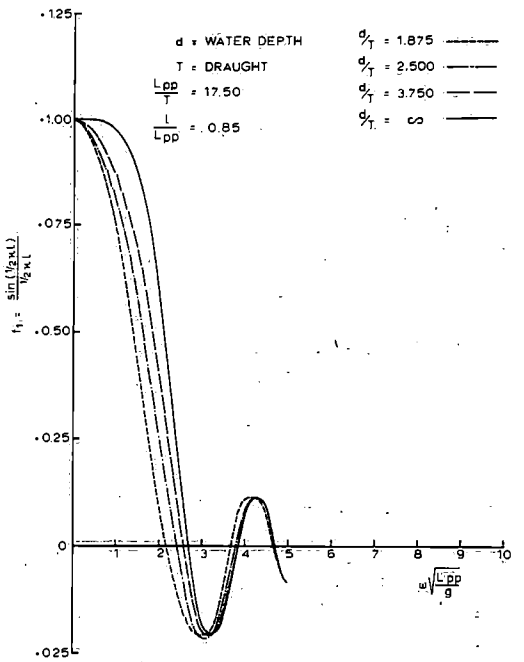

Fig. 15. Influence of water depth on the factor $f_1 = \{\sin(\frac{1}{2}\kappa l)\}/(\frac{1}{2}\kappa l)$ in which l is taken to be $0.85 L_{pp}$.

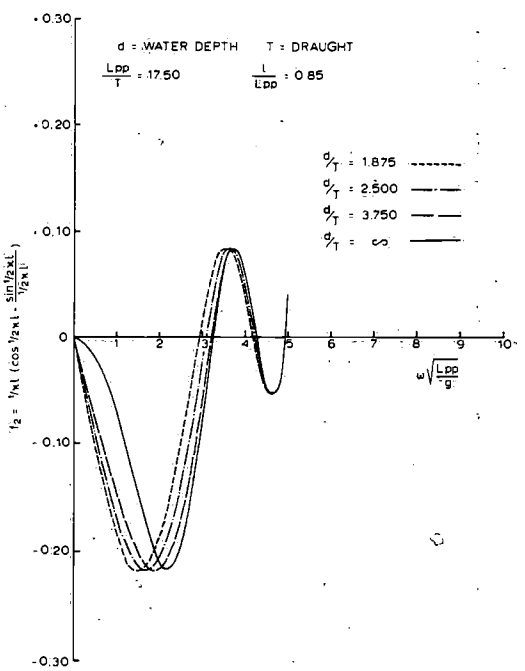

Fig. 16. Influence of water depth on the factor $f_2 = 1/\kappa l\,[\cos(\frac{1}{2}\kappa l) - \{\sin(\frac{1}{2}\kappa l)\}/(\frac{1}{2}\kappa l)]$ in which l is taken to be $0.85 L_{pp}$.

In figure 13 the frequencies at which factor f_1 in figure 15 becomes zero have been indicated. It can be seen that these values correspond well with the frequencies at which the wave excited vertical forces become minimal.

Referring to the frequency mentioned under the above item *b* the location *c* of the minimum value in figure 13 can be explained by the fact that at a given cross section of the ship the wave force per unit length Z'_a (see equation 11) becomes minimal because the wave excited inertia force and the wave excited Froude-Krilov force cancel each other. These components of the total wave excited force per unit length amount to

$$Z'_{1(t)} = +\mu_1 \varrho g B \zeta_a \sin(\omega t) \tag{13}$$

for the Froude-Krilov contribution

$$Z'_{2(t)} = -\mu_2 a'_{zz} \omega^2 \zeta_a \sin(\omega t) \tag{14}$$

for the inertia force.

in which

κ = wave number
ω = wave circular frequency
ζ = wave amplitude
T = ship's draught
B = ship's breadth
a'_{zz} = vertical added mass per unit length

$$\mu_1 = \frac{\cosh(d-T)}{\cosh \kappa d} \to e^{-\kappa T} \quad \text{if} \quad d \to \infty$$

$$\mu_2 = \frac{\sinh(d-T)}{\sinh \kappa d} \to e^{-\kappa T} \quad \text{if} \quad d \to \infty$$

d = water depth

From figure 8 a natural heave frequency of about $3.1\sqrt{g/L}$ is found from which also the added mass a_{zz} of the ship is obtained.

Combining equations (13) and (14) it will be found that in deep water the vertical wave excited force will be minimal at about

$$\omega_c = \omega_z \sqrt{\frac{M + a_{zz}}{a_{zz}}} \tag{15}$$

in which
ω_z = natural heave frequency
M = mass of ship

For the ship being studied it is found from fig. 13 that

$$\omega_c = 4.35\sqrt{g/L_{pp}}$$

From the above given analysis of the wave-excited force it will be obvious that the influence of the water depth on the wave excited force is felt in several ways:

1. Due to a change of the coefficients μ_1 and μ_2 (see equation (13) and (14)) the pressure variation (Froude-Krilov force) and the inertia forces will change the amplitude of the wave excited force at some locations of the ship according to figure 17.
2. Due to a change of the added mass at a changing water depth, the inertia force will change (see equation (14)) on account of which the wave excited force at some locations of the ship will change. However, the influence of the waterdepth on the added mass can be neglected when the water depth is more than two times the draught as is the case in the present study.
3. Due to a change of wave length at the same wave frequency the effective wave excited force will change at a varying water depth as can be seen from figure 15 and 16.

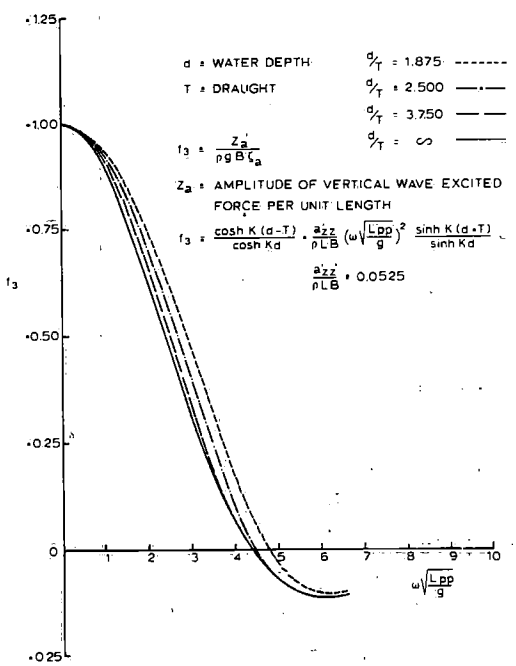

Fig. 17. Influence of water depth on the amplitude of the dimensionless vertical wave excited force per unit length of the ship.

7 Motions of a ship in waves at restricted water depth

In figures 18 and 19 the heave and pitch motions of the ship being studied are given for deep water. These motions are a result of the above discussed reaction and exciting forces (see equations (8) and (9)) as will be elucidated in the following. From figure 8 it follows that he natural heave frequency amounts to $3.1\sqrt{g/L_{pp}}$ rad/sec. For zero speed the dimensionless reaction function at this natural frequency amounts to 4.42 according to figure 8. According to figure 13 the dimensionless wave excited force amounts to 0.095

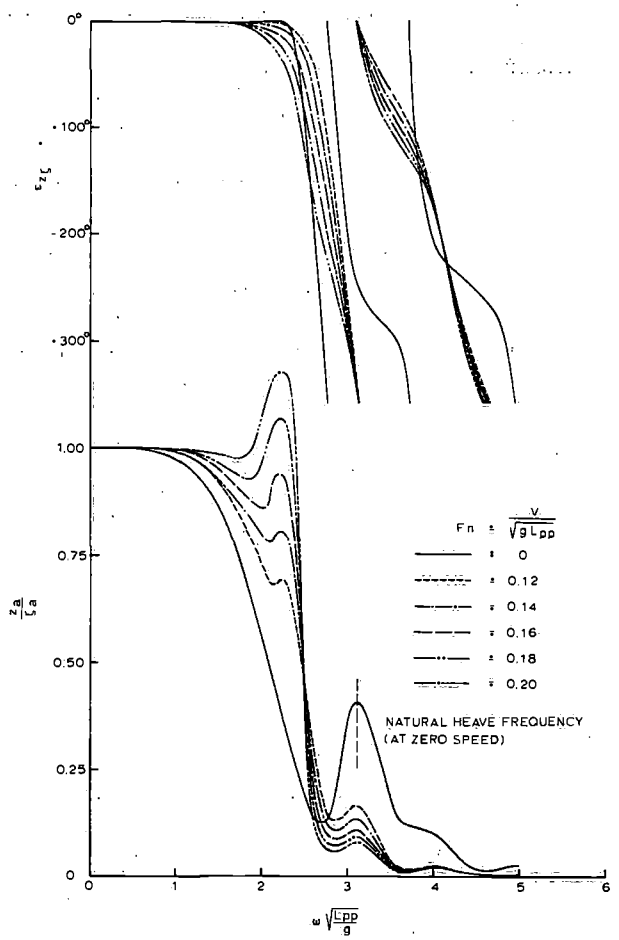

Fig. 18. Influence of ship speed on heave response function for deep water.

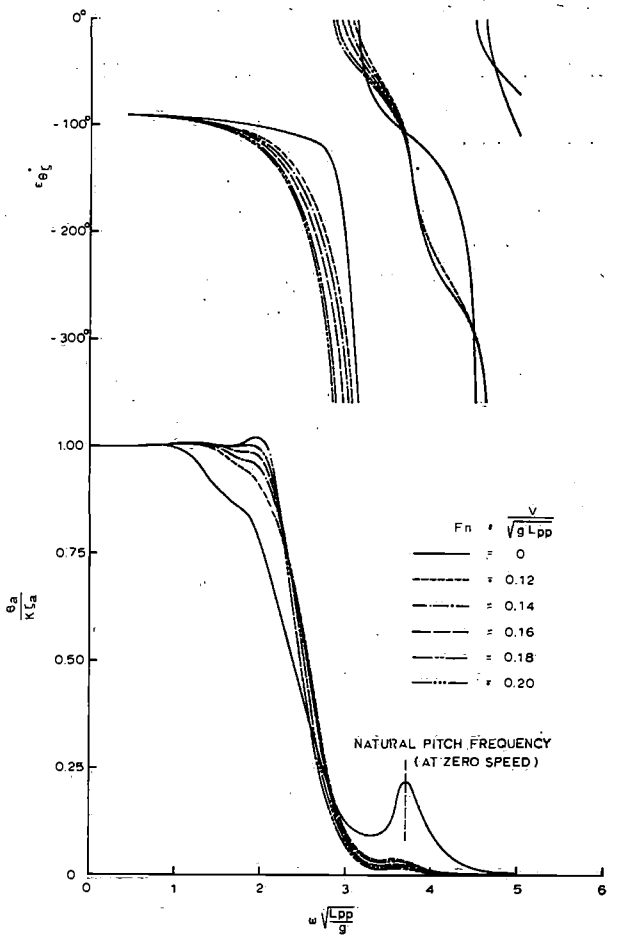

Fig. 19. Influence of ship speed on pitch response function for deep water.

at the wave frequency of $3.1\sqrt{g/L_{pp}}$ rad/sec. The heave response to waves therefore amounts to 0.42 which corresponds to the peak value at $\omega = 3.1\sqrt{g/L_{pp}}$ rad/sec in figure 18 for zero speed of the ship.

At increasing ship speeds the frequency of encounter corresponding to the wave frequency of $3.1\sqrt{g/L_{pp}}$ rad/sec, will increase as indicated in figure 7. At increasing frequencies of encounter the reaction function will decrease according to figure 8. From this the reduction of heave response for wave frequencies of $3.1\sqrt{g/L_{pp}}$ rad/sec at increasing ship speeds can be explained.

In the same way the reduction of the wave frequency at which the heave response has a maximum value can be deduced from the increment of the ship speed.

Taking the earlier findings into account the ship motions a restricted water depths can now be deduced from the ship motions in deep water (see Appendix I).

8 Conclusions

The motions of a ship sailing at restricted water depths can be deduced from the ship motions at deep water. This statement is based on the following conclusions

1. The reaction forces at a given frequency of oscillation of the ship will hardly be influenced by the water depth if this depth is greater than about two times the ship's draught ($d > 2T$).
2. Due to the restricted water depth the wave frequency will change when a given frequency of ship oscillation is regarded (figure 7).
3. Due to the restricted water depth the relationship between wave length and wave frequency will change, on account of which at a given wave frequency the wave excited force or moment will change accordingly (figures 15 and 16).
4. Due to the restricted water depth the wave action will increase at a given wave period, on account of which the wave excited force will change accordingly (figure 17).

References

1. VUGTS, J. H., The hydrodynamic forces and ship motions in waves, Thesis of the Technical University Delft 1970.
2. KIM, C. H., The influence of water depth on the heaving and pitching motions of a ship moving in longitudinal regular head waves, Chalmers University of Technology, Division of Ship Hydromechanics, Report No. 44, Göteborg 1968.
3. FREAKES, W. and K. L. KEAY, Effects of shallow water on ship motion parameters in pitch and heave, M.I.T. Department of Naval Architecture and Marine Engineering – Report No. 66-7, Cambridge 1966.
4. TUCK, E. O. and R. J. Taylor, Shallow water problems in ship hydrodynamics, 8th Symposium on Naval Hydrodynamics, Pasadena 1970.
5. VERMEER, H., Gedrag van een schip in beperkt water, M.S. thesis, Technical University Delft.
6. STUMPF, V. M. et al., A study of hull form effects on the resistance of large tankers, International Marine and Shipping Conference, London 1969.
7. BAZILEVSKY, Y. S. et al., Modern means to control flow separation on full model forms, 12th International Towing Tank Conference, Rome 1969.
8. HOOFT, J. P., The dynamical behaviour of a floating drilling platform, Report of the Post Graduate Course, May 1969, H. Veenman en Zonen N.V. Wageningen.
9. TASAI, F. and C. H. KIM, Effect of shallow water on the natural period of heave, Research Institute of Applied Mechanics, Kyushu University, Volume XVI, No. 54, 1968.
10. FLOKSTRA, C., Ship motions in regular waves, Report No. 70-229-WO, Netherlands Ship Model Basin Wageningen, 1973.

APPENDIX I

Determination of the motions of ships sailing at restricted water depths

According to equation (9) one finds for the heave motion

$$\frac{z_a}{\zeta_a} e^{i\varepsilon_z} = A_1 e^{i\alpha_1} \frac{Z_a}{\zeta_a} e^{i\sigma_z} + B_1 e^{i\beta_1} \frac{M_a}{\zeta_a} e^{i\sigma_M} \tag{1A}$$

in which the wave excited vertical force Z_a and pitching moment M_a depend on the wave frequency. Since the heave motion z_a has to be determined for some frequency ω_e, ω_e as a function of ω and the ship speed (see figure 7) is first determined.

$$\omega = \omega_e - V\kappa \cos\mu \tag{2A}$$

The wave excited force at some waterdepth d now follows from equation (12)

$$Z_{(d)} = Z_{(\infty)} \cdot \frac{f_{1(d)} \cdot f_{3(d)}}{f_{1(\infty)} \cdot f_{3(\infty)}} \tag{3A}$$

in which the subscript ∞ indicates the values at infinite deep water. The values f_1 and f_3 are given in figure 15 resp. figure 17.

In the same way one finds

$$M_d = M_{(\infty)} \cdot \frac{f_{2(d)} \cdot f_{3(d)}}{f_{2(\infty)} \cdot f_{3(\infty)}} \tag{4A}$$

in which f_2 follows from figure 16.

Once Z and M are known one determines $A_1 e^{i\alpha_1}$ and $B_1 e^{i\beta_1}$ from figures 8 and 9. The amplitude of the heave motion then follows from

$$z_a = \sqrt{z_1^2 + z_2^2} \tag{5A}$$

in which

$$z_1 = z_a \cos\varepsilon_z = A_1 Z_a \cos(\alpha_1 + \sigma_z) + B_1 M_a \cos(\beta_1 + \sigma_M)$$

$$z_2 = z_a \sin\varepsilon_z = A_1 Z_a \sin(\alpha_1 + \sigma_z) + B_1 M_a \sin(\beta_1 + \sigma_M)$$

The phase difference ε_z follows from

$$\varepsilon_z = \arctan z_2/z_1$$

In the same way one finds for the pitch motion

$$\theta_a = \sqrt{\theta_1^2 + \theta_2^2} \tag{6A}$$

$$\varepsilon_\theta = \arctan \theta_2/\theta_1$$

in which

$$\theta_1 = \theta_a \cos\varepsilon_\theta = A_2 Z_a \cos(\alpha_2 + \sigma_z) + B_2 M_a \cos(\beta_2 + \sigma_M)$$

$$\theta_2 = \theta_a \sin\varepsilon_\theta = A_2 Z_a \sin(\alpha_2 + \sigma_z) + B_2 M_a \sin(\beta_2 + \sigma_M)$$

In figures 20 to 29 the heave and pitch motions as measured earlier are given in comparison with the estimated values according to equation (5A) and (6A).

APPENDIX II

Measurements of thrust and power

During the model tests the thrust and power have also been measured. In figure 30 the thrust and power deduced from the self propulsion model test (without skin friction correction) are presented. From figure 30 the thrust and power prediction for full scale (a skin friction correction being used) have been determined and presented in figure 31.

From figures 30 and 31 it can be seen that the effect of the water depth becomes only noticeable at higher ship speeds. For the prediction of the thrust and power in waves from the results of the model tests, use is made of the assumption (π_h-method), that

$$P_S = P_w - P_0 - P_p \quad \text{and} \quad T_S = T_w - T_0 + T_p$$

in which

P_w and T_w are the power and the thrust in waves without skin friction correction.

P_S and T_S are the power and the thrust with the friction correction.

P_0 and T_0 are the power and the thrust in smooth water without skin friction correction.

P_p and T_p are the power and the thrust in smooth water with skin friction correction.

The power increase and the thrust increase due to waves are

$$P_h = P_w - P_0$$

$$T_h = T_w - T_0$$

These increases were made dimensionless as follows

$$\pi_h = \frac{P_h}{\varrho g \zeta_a^2 (B^2/L_{pp}) \cdot V}$$

$$\tau_h = \frac{T_h}{\varrho g \zeta_a^2 (B^2/L_{pp})}$$

These dimensionless values are plotted in figures 32 through 37 on base of Froude number for various values of $\omega\sqrt{L_{pp}/g}$.

As can be seen the largest thrust and power increases generally occur for a value of $\omega\sqrt{L_{pp}/g} = 2.285$.

This is valid over a large range of Froude numbers and for each water depth investigated.

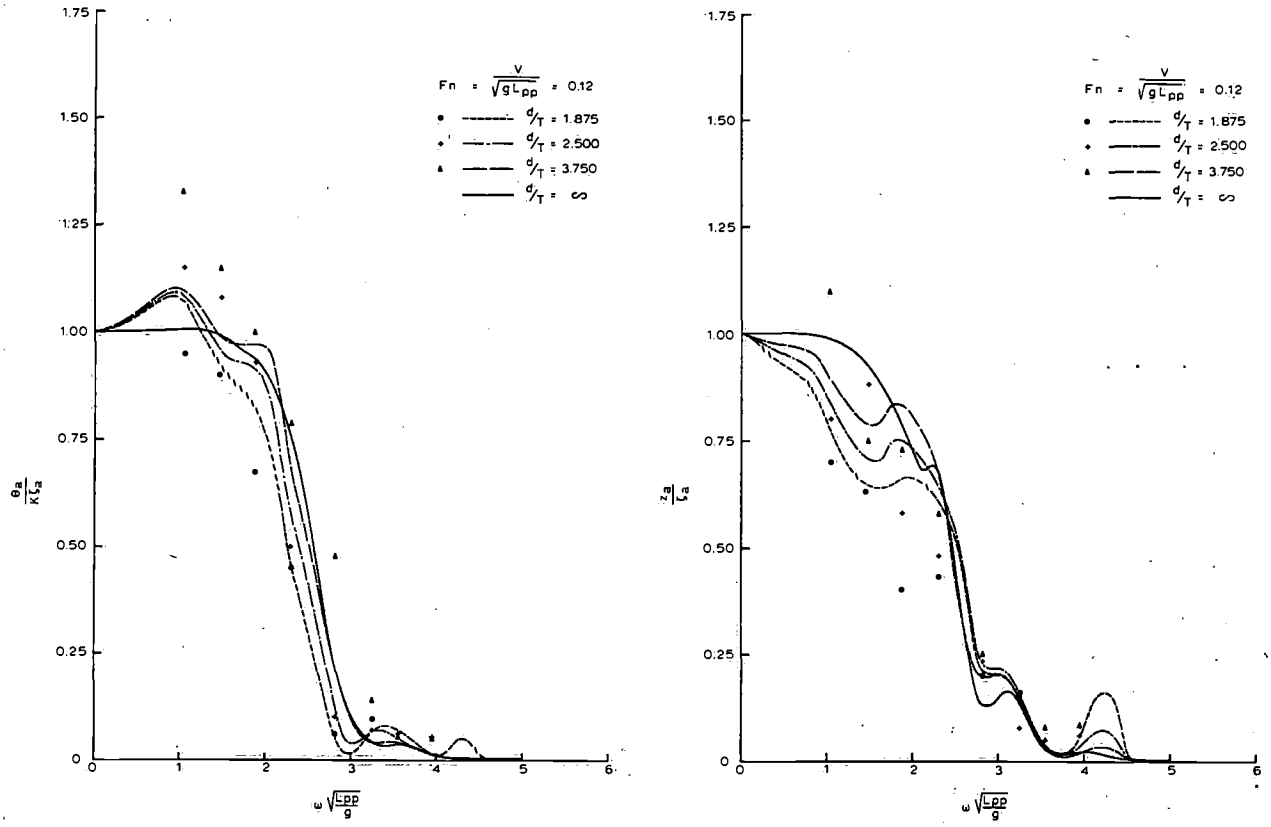

Fig. 20. Comparison of estimated and measured heave and pitch motions as a function of the water depth at Froude number 0.12.

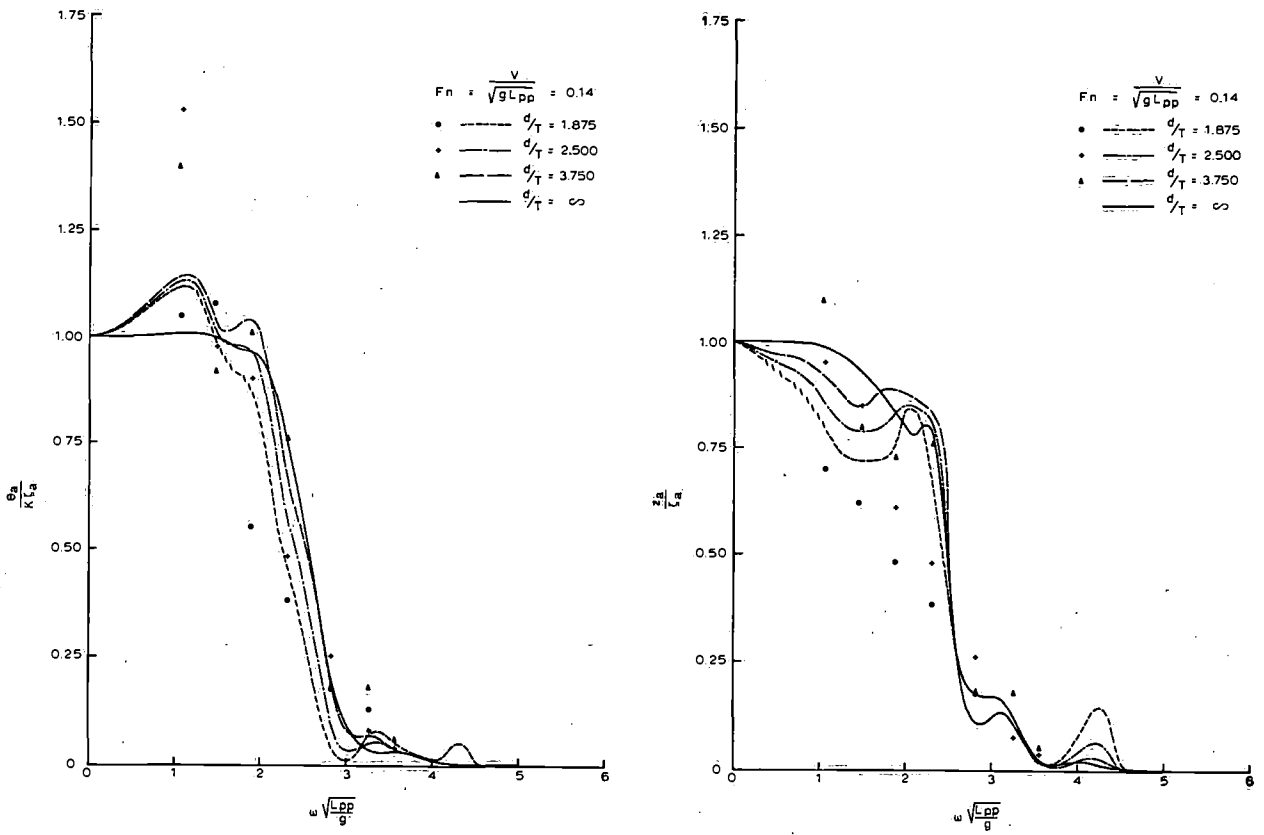

Fig. 21. Comparison of estimated and measured heave and pitch motions as a function of the water depth at Froude number 0.14.

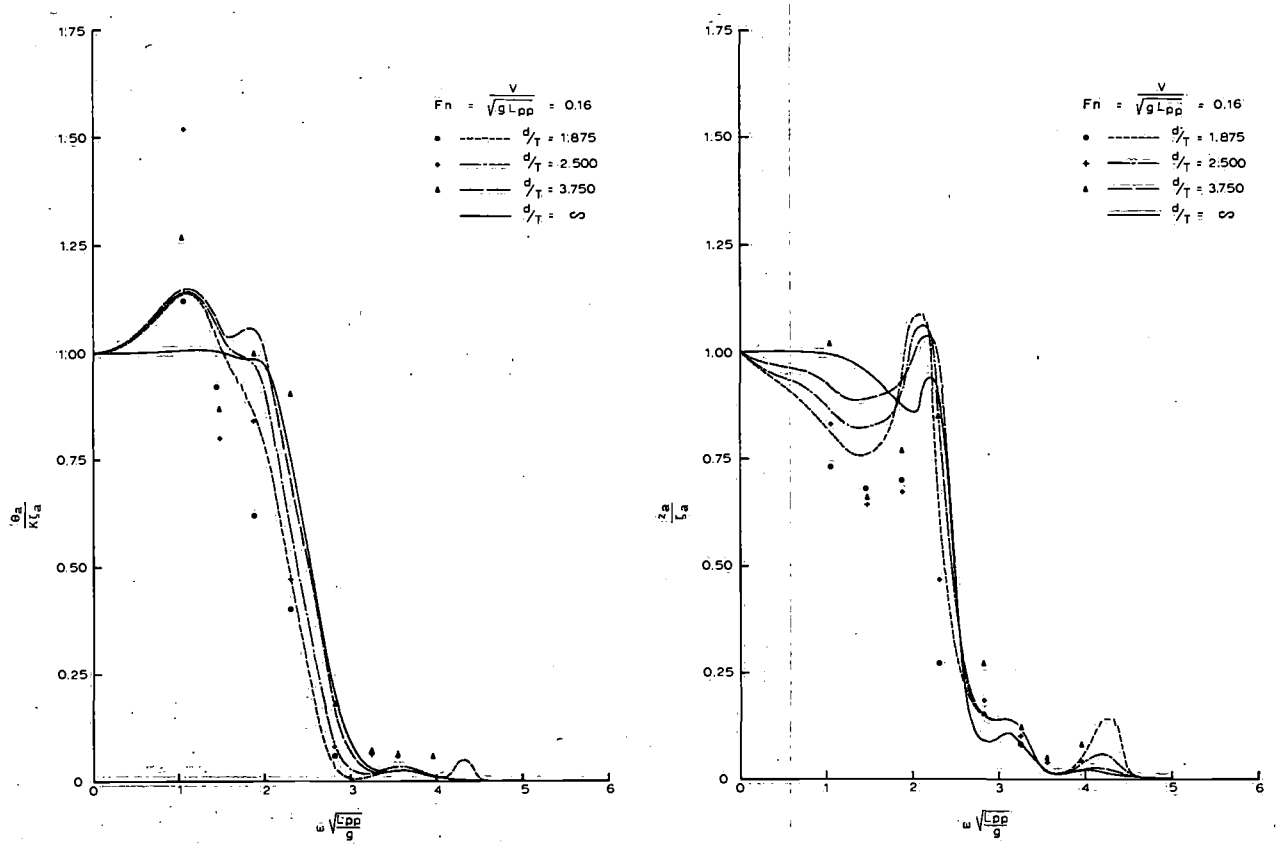

Fig. 22. Comparison of estimated and measured heave and pitch motions as a function of the water depth at Froude number 0.16.

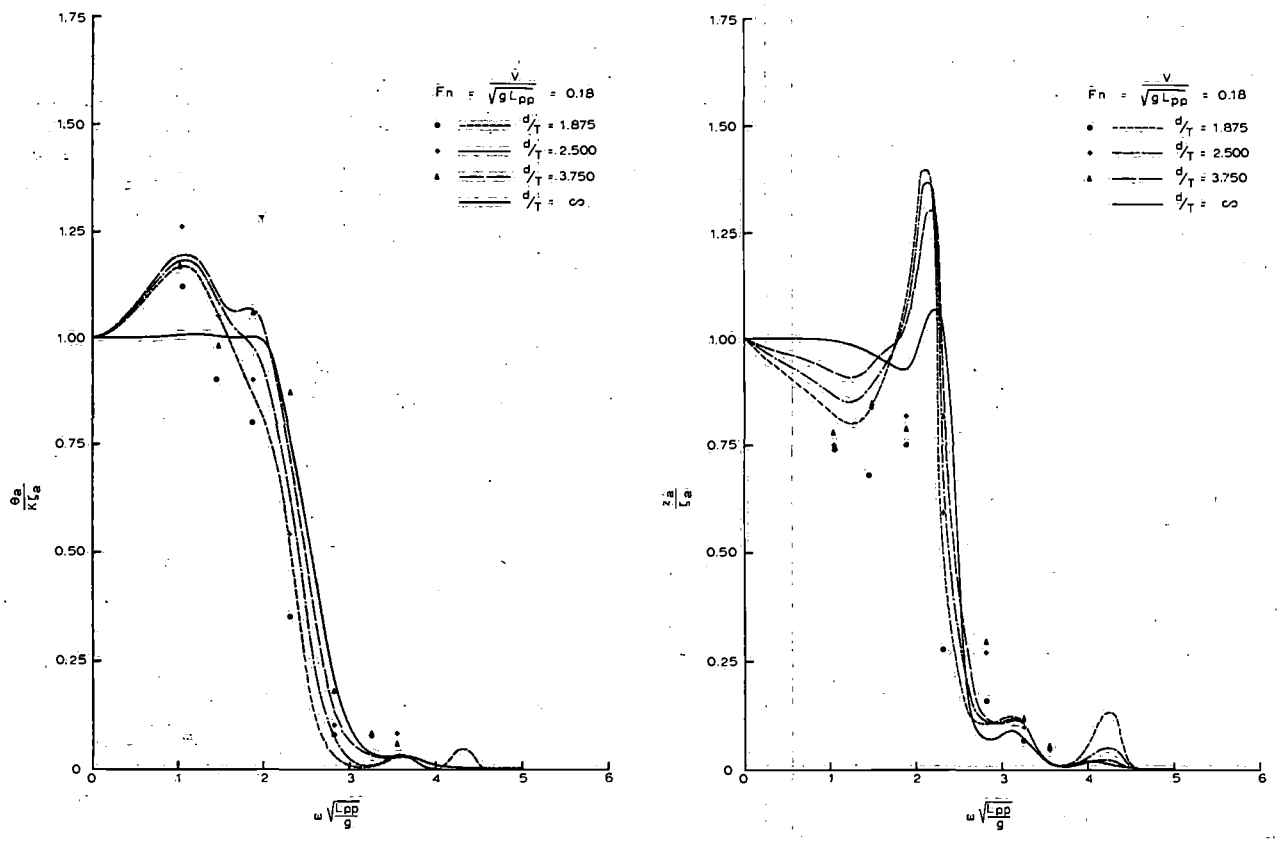

Fig. 23. Comparison of estimated and measured heave and pitch motions as a function of the water depth at Froude number 0.18.

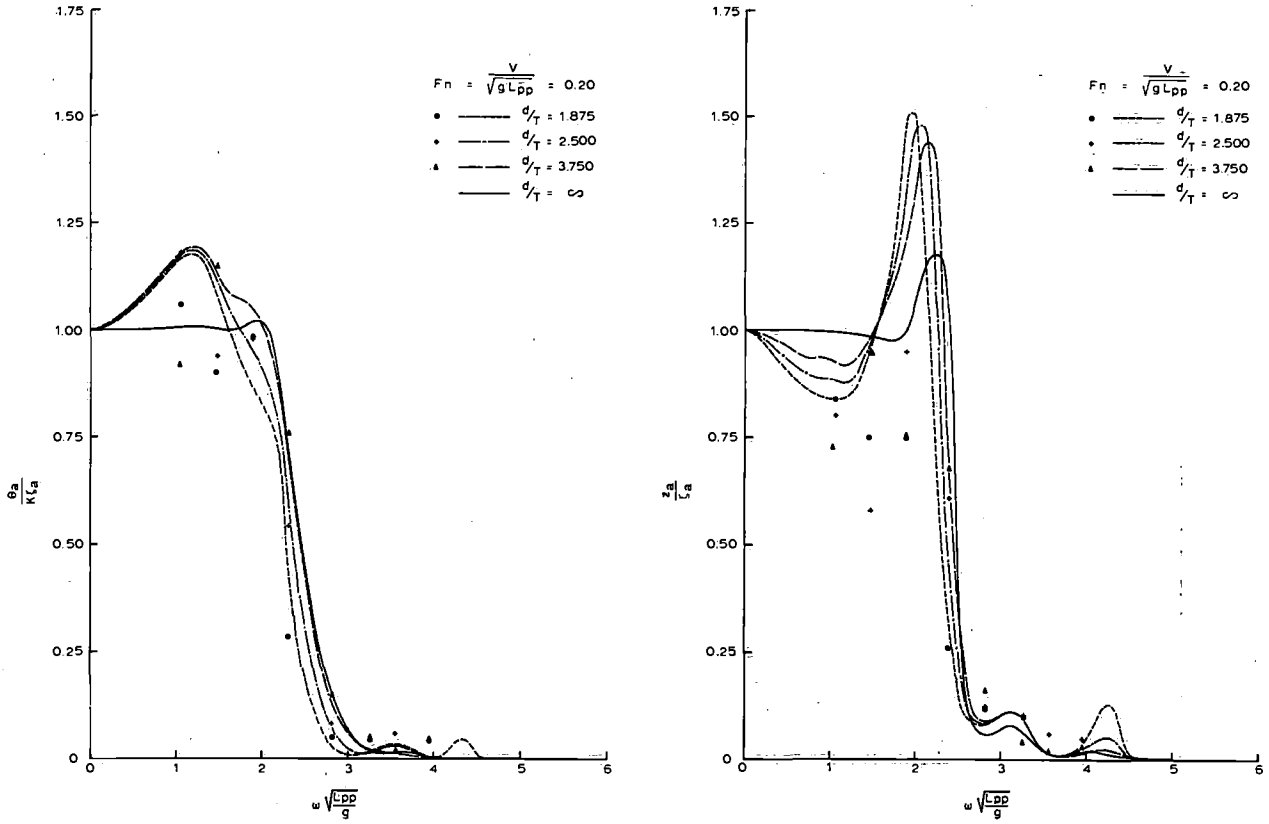

Fig. 24. Comparison of estimated and measured heave and pitch motions as a function of the water depth at Froude number 0.20.

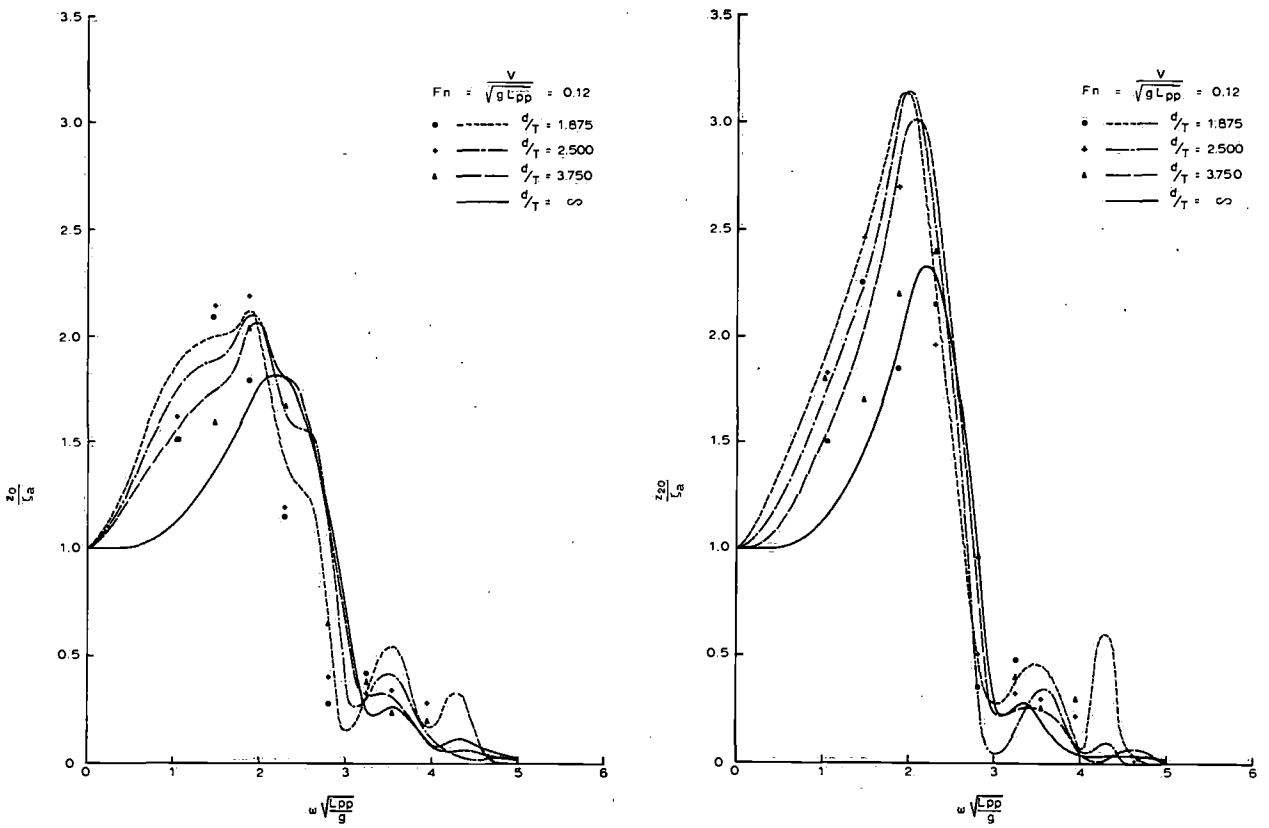

Fig. 25. Comparison of estimated and measured vertical motions of the bow and stern as a function of the water depth at Froude number 0.12.

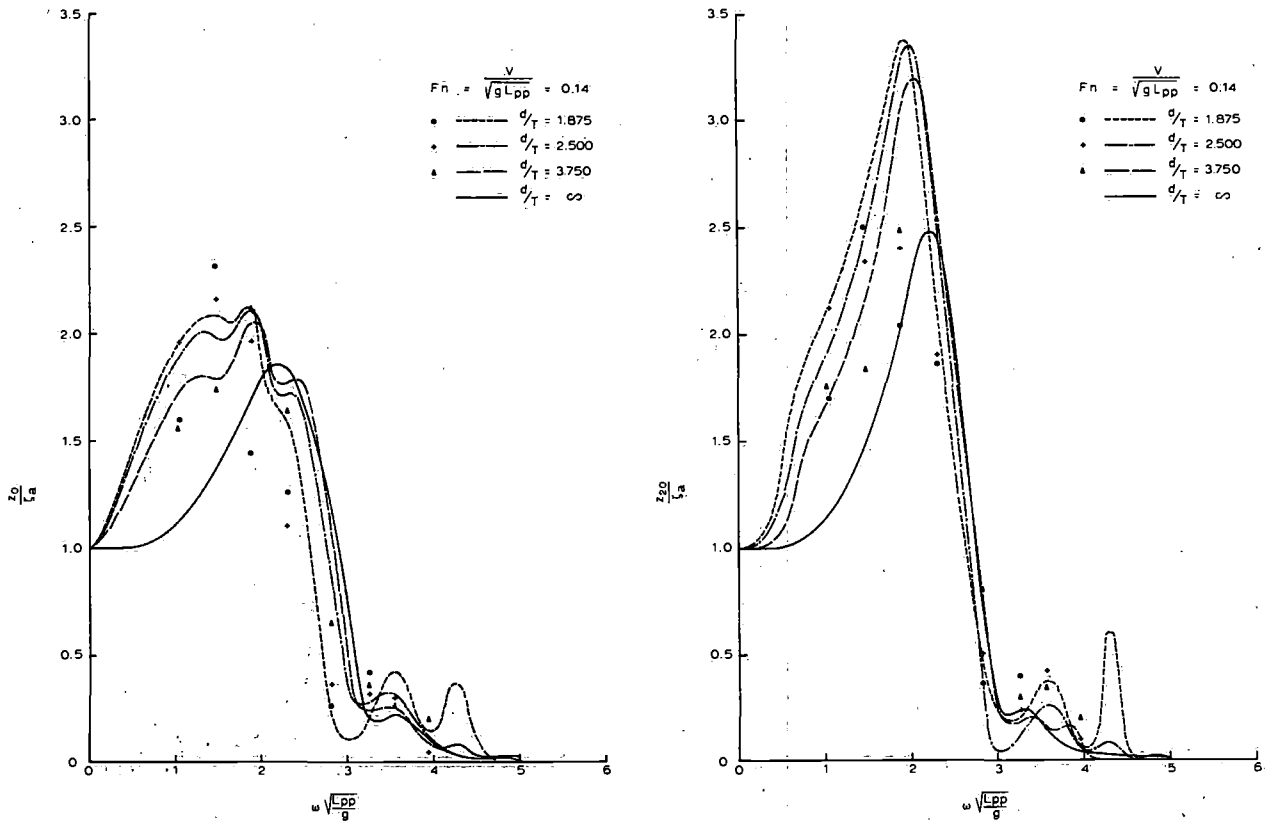

Fig. 26. Comparison of estimated and measured vertical motions of the bow and stern as a function of the water depth at Froude number 0.14.

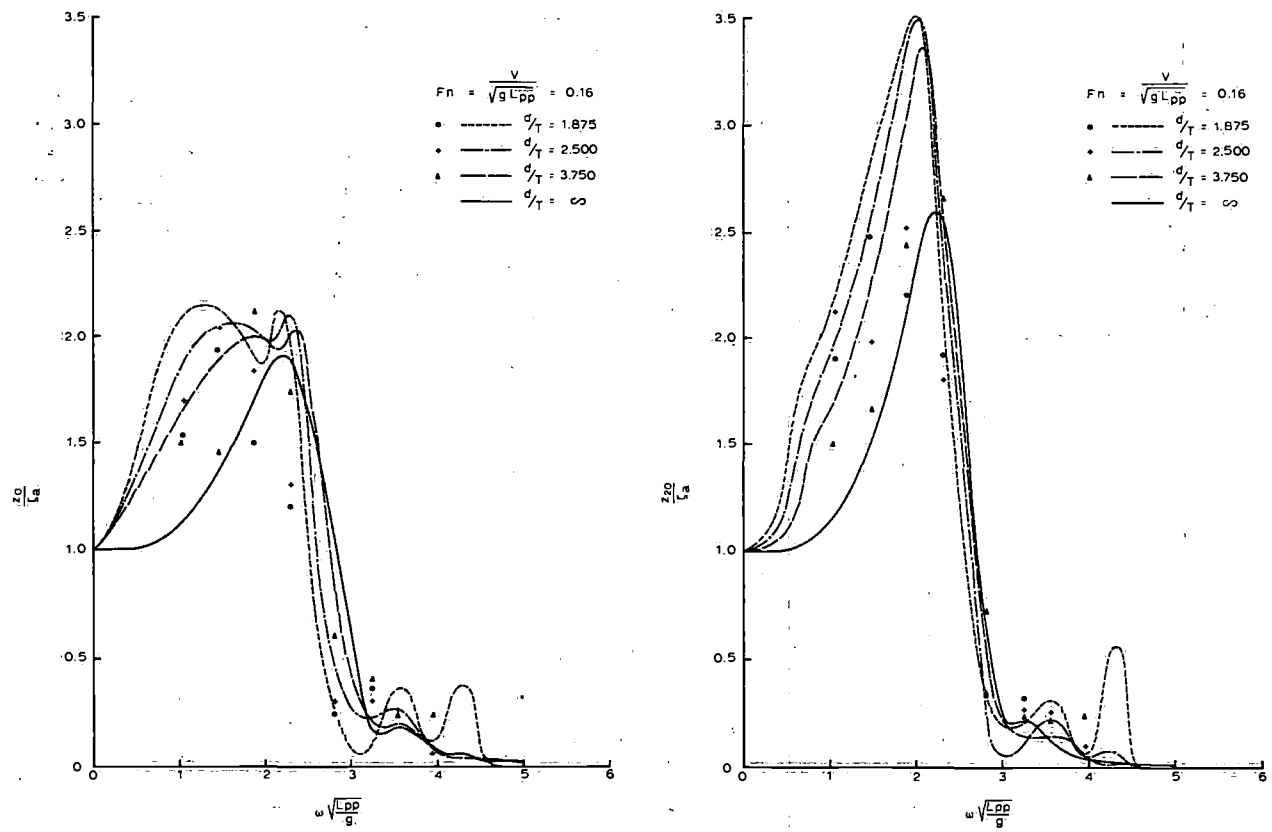

Fig. 27. Comparison of estimated and measured vertical motions of the bow and stern as a function of the water depth at Froude number 0.16.

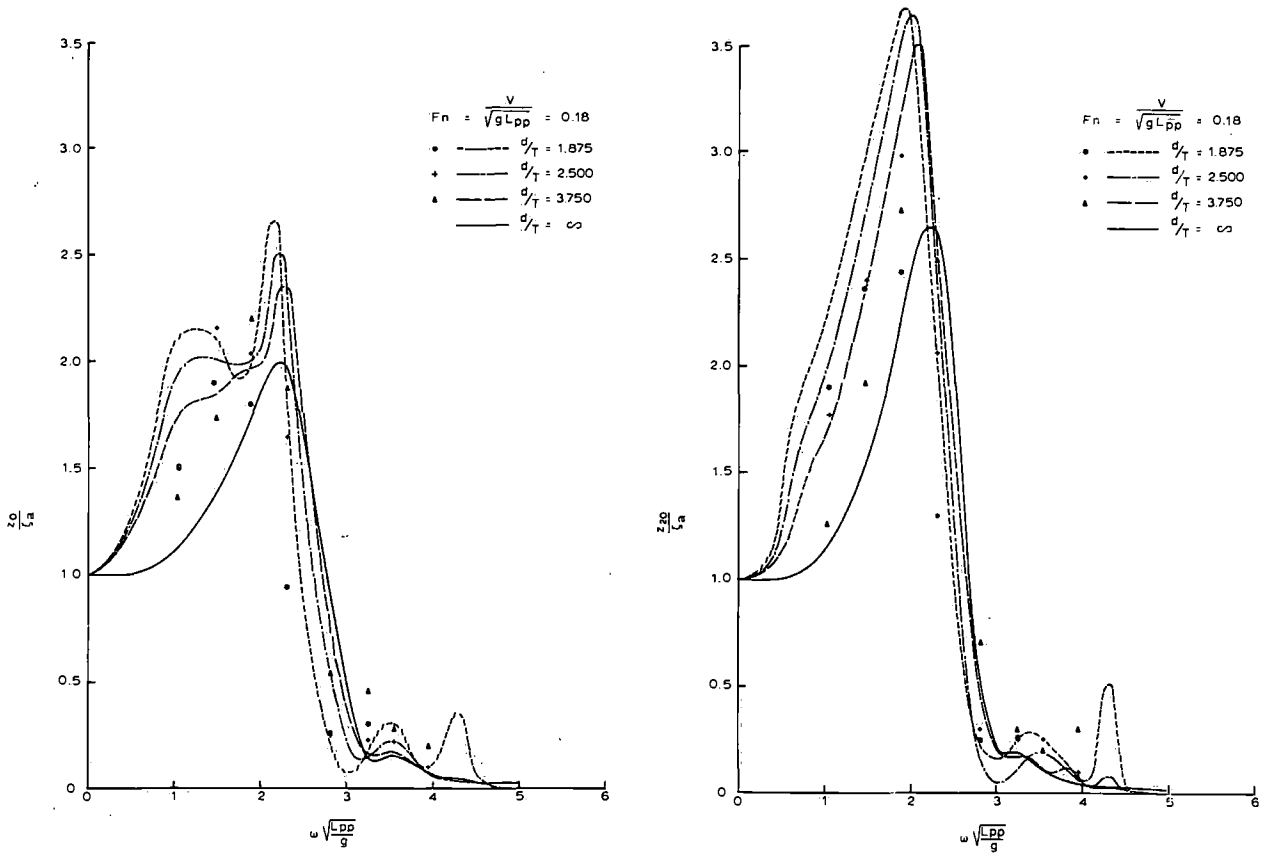

Fig. 28. Comparison of estimated and measured vertical motions of the bow and stern as a function of the water depth at Froude number 0.18.

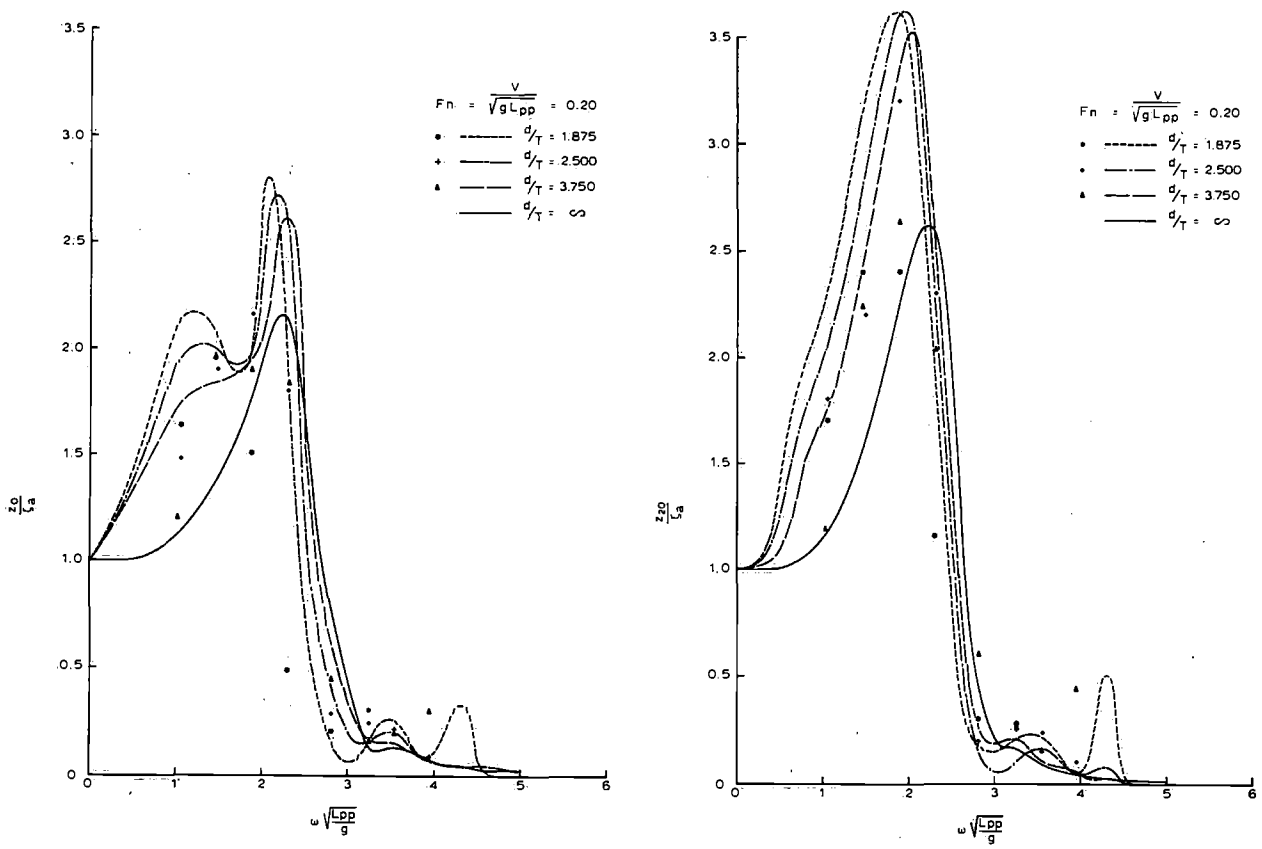

Fig. 29. Comparison of estimated and measured vertical motions of the bow and stern as a function of the water depth at Froude number 0.20.

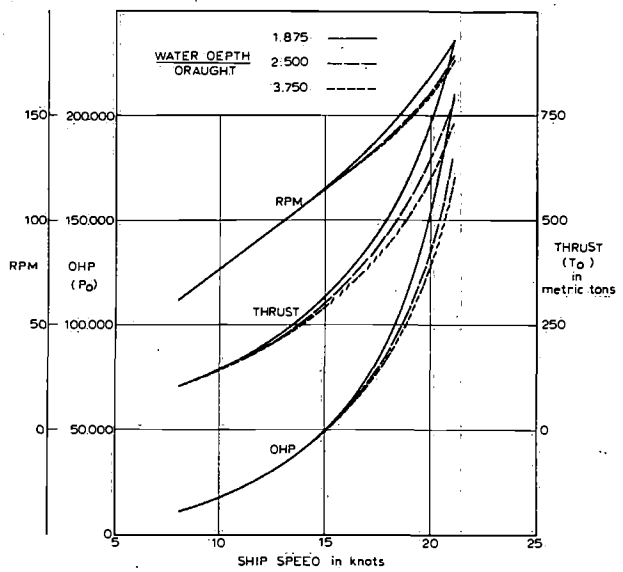

Fig. 30. Power-thrust-speed relationship for smooth water in the self-propulsion condition of a 100,000 TDW tanker.

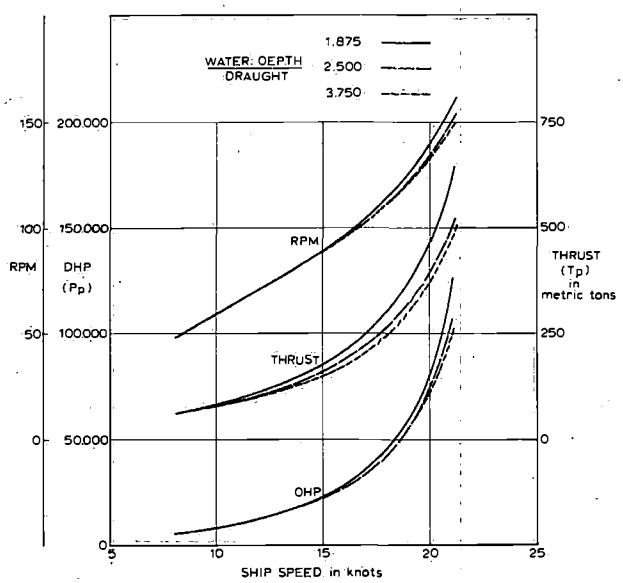

Fig. 31. Power-thrust-speed relationship for smooth water in the self-propulsion condition of model.

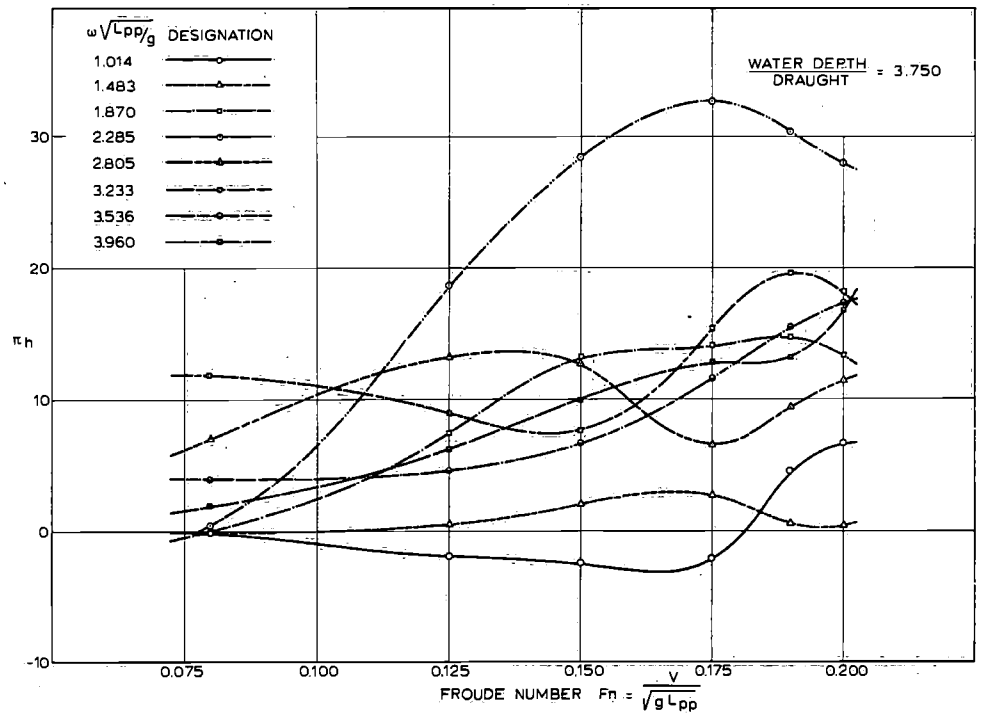

Fig. 32. Dimensionless power increase due to waves as a function of the Froude number and the wave frequency for a water depth of 3.75× draught.

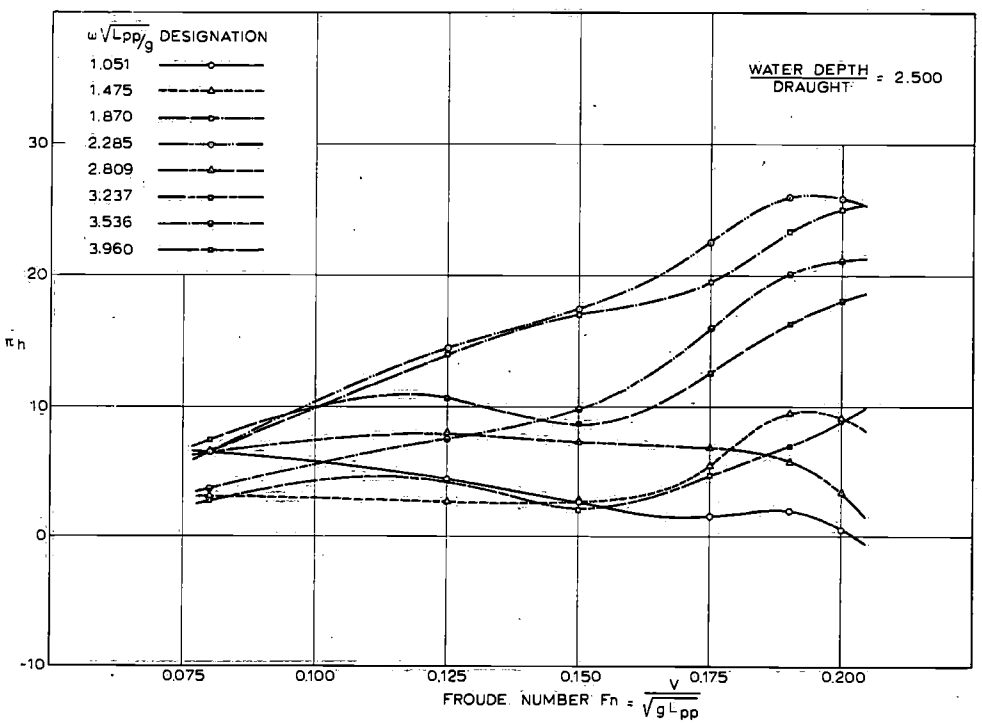

Fig. 33. Dimensionless power increase due to waves as a function of the Froude number and the wave frequency for a water depth of 2.5× draught.

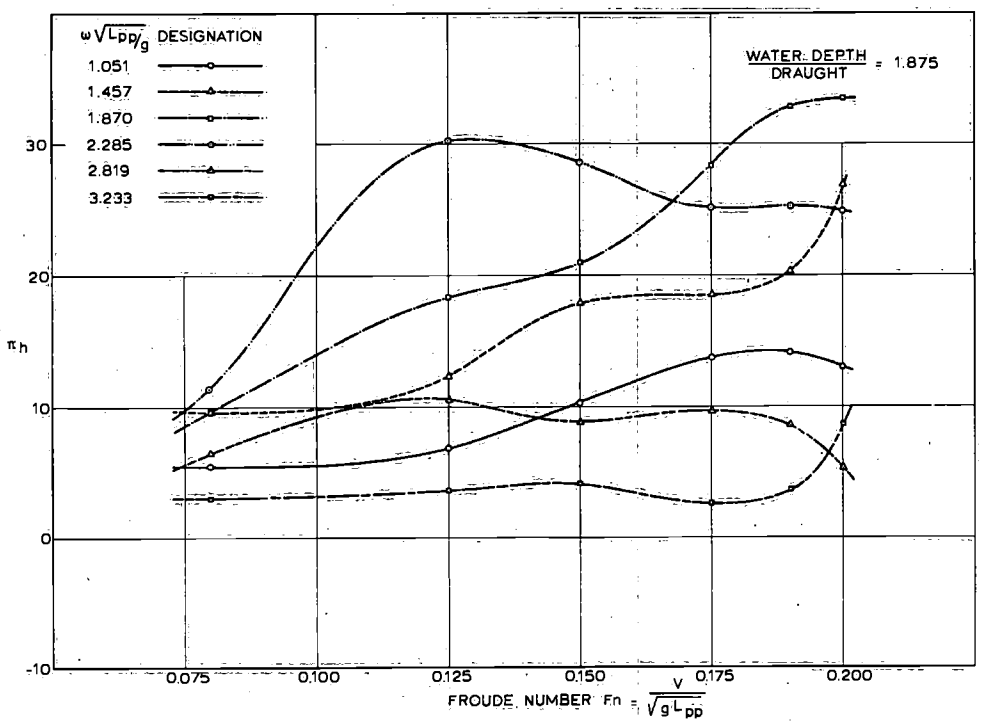

Fig. 34. Dimensionless power increase due to waves as a function of the Froude number and the wave frequency for a water depth of 1.875× draught.

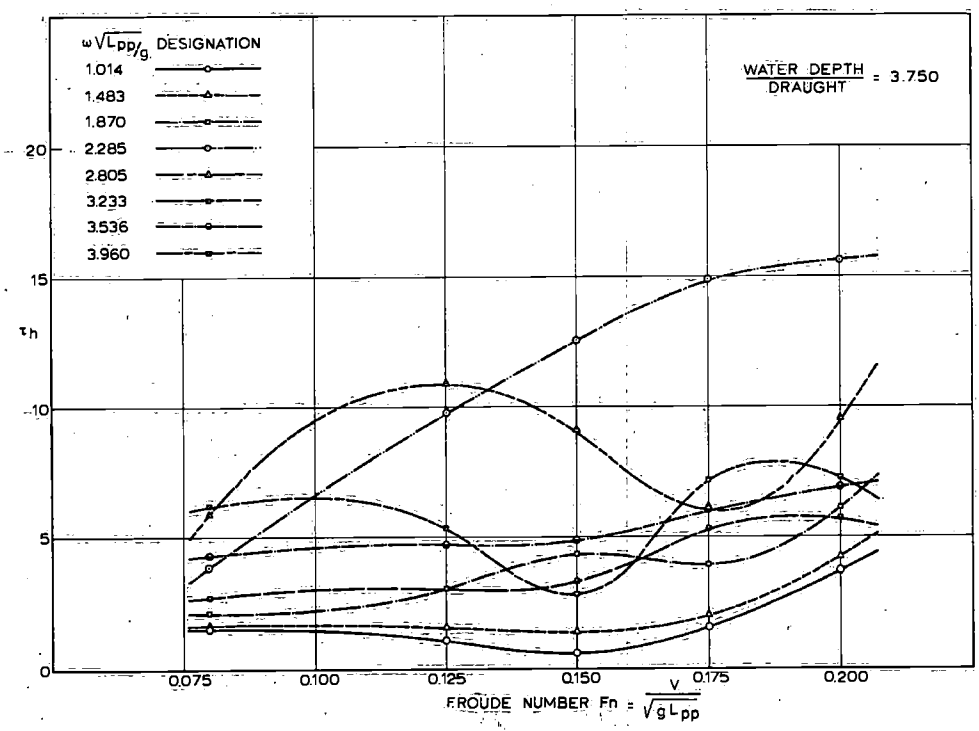

Fig. 35. Dimensionless thrust increase due to waves as a function of the Froude number and the wave frequency for a water depth of 3.75× draught.

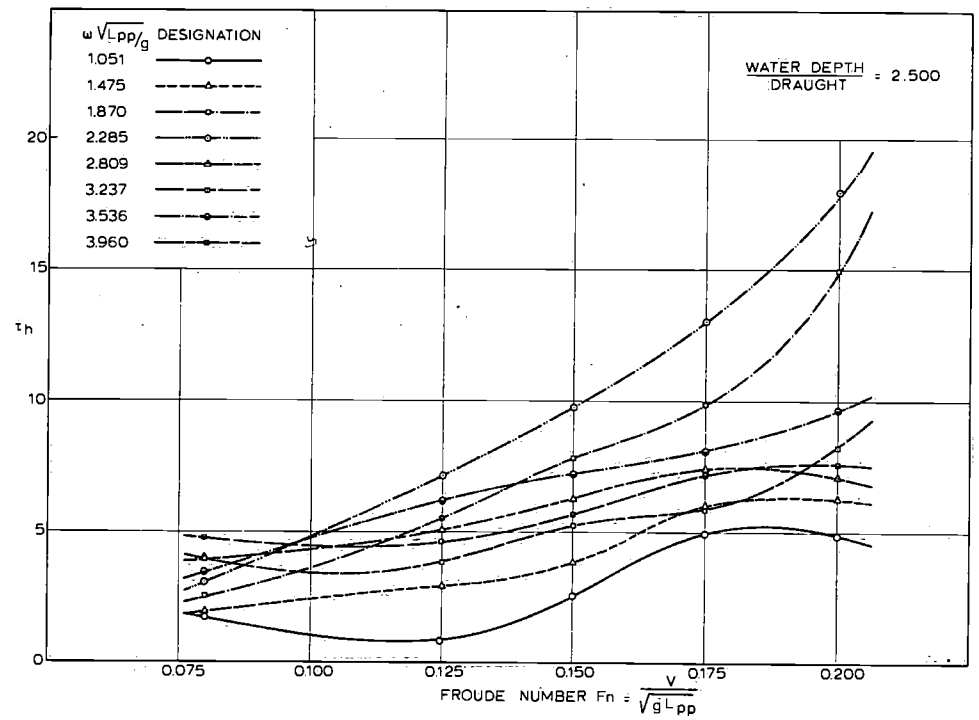

Fig. 36. Dimensionless thrust increase due to waves as a function of the Froude number and the wave frequency for a water depth of 2.5× draught.

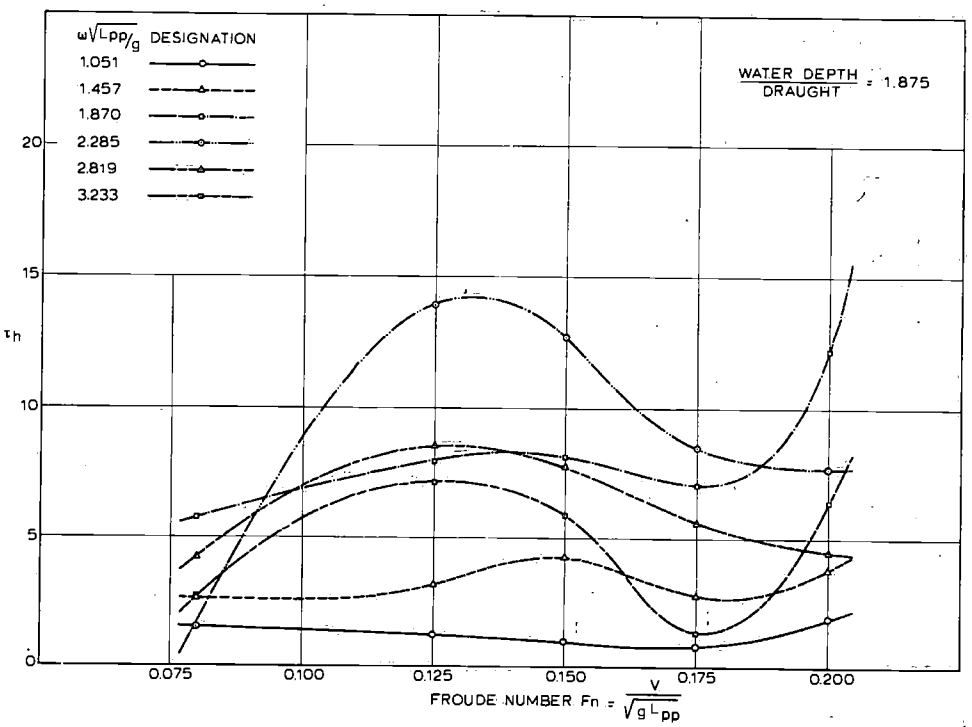

Fig. 37. Dimensionless thrust increase due to waves as a function of the Froude number and the wave frequency for a water depth of 1.875× draught.

PUBLICATIONS OF THE NETHERLANDS SHIP RESEARCH CENTRE TNO

LIST OF EARLIER PUBLICATIONS AVAILABLE ON REQUEST
PRICE PER COPY DFL. 10.— (POSTAGE NOT INCLUDED)

M = engineering department S = shipbuilding department C = corrosion and antifouling department

Reports

90 S Computation of pitch and heave motions for arbitrary ship forms. W. E. Smith, 1967.
91 M Corrosion in exhaust driven turbochargers on marine diesel engines using heavy fuels. R. W. Stuart Mitchell, A. J. M. S. van Montfoort and V. A. Ogale, 1967.
92 M Residual fuel treatment on board ship. Part II. Comparative cylinder wear measurements on a laboratory diesel engine using filtered or centrifuged residual fuel. A de Mooy, M. Verwoest and G. G. van der Meulen, 1967.
93 C Cost relations of the treatments of ship hulls and the fuel consumption of ships. H. J. Lageveen-van Kuijk, 1967.
94 C Optimum conditions for blast cleaning of steel plate. J. Remmelts, 1967.
95 M Residual fuel treatment on board ship. Part I. The effect of centrifuging, filtering and homogenizing on the unsolubles in residual fuel. M. Verwoest and F. J. Colon, 1967.
96 S Analysis of the modified strip theory for the calculation of ship motions and wave bending moments. J. Gerritsma and W. Beukelman, 1967.
97 S On the efficacy of two different roll-damping tanks. J. Bootsma and J. J. van den Bosch, 1967.
98 S Equation of motion coefficients for a pitching and heaving destroyer model. W. E. Smith, 1967.
99 S The manoeuvrability of ships on a straight course. J. P. Hooft, 1967.
100 S Amidships forces and moments on a $C_B = 0.80$ "Series 60" model in waves from various directions. R. Wahab, 1967.
101 C Optimum conditions for blast cleaning of steel plate. Conclusion. J. Remmelts, 1967.
102 M The axial stiffness of marine diesel engine crankshafts. Part I. Comparison between the results of full scale measurements and those of calculations according to published formulae. N. J. Visser, 1967.
103 M The axial stiffness of marine diesel engine crankshafts. Part II. Theory and results of scale model measurements and comparison with published formulae. C. A. M. van der Linden, 1967.
104 M Marine diesel engine exhaust noise. Part I. A mathematical model. J. H. Janssen, 1967.
105 M Marine diesel engine exhaust noise. Part II. Scale models of exhaust systems. J. Buiten and J. H. Janssen, 1968.
106 M Marine diesel engine exhaust noise. Part III. Exhaust sound criteria for bridge wings. J. H. Janssen en J. Buiten, 1967.
107 S Ship vibration analysis by finite element technique. Part I. General review and application to simple structures, statically loaded. S. Hylarides, 1967.
108 M Marine refrigeration engineering. Part I. Testing of a decentralised refrigerating installation. J. A. Knobbout and R. W. J. Kouffeld, 1967.
109 S A comparative study on four different passive roll damping tanks. Part I. J. H. Vugts, 1968.
110 S Strain, stress and flexure of two corrugated and one plane bulkhead subjected to a lateral, distributed load. H. E. Jaeger and P. A. van Katwijk, 1968.
111 M Experimental evaluation of heat transfer in a dry-cargo ships' tank, using thermal oil as a heat transfer medium. D. J. van der Heeden, 1968.
112 S The hydrodynamic coefficients for swaying, heaving and rolling cylinders in a free surface. J. H. Vugts, 1968.
113 M Marine refrigeration engineering. Part II. Some results of testing a decentralised marine refrigerating unit with R 502. J. A. Knobbout and C. B. Colenbrander, 1968.
114 S The steering of a ship during the stopping manoeuvre. J. P. Hooft, 1969.
115 S Cylinder motions in beam waves. J. H. Vugts, 1968.
116 M Torsional-axial vibrations of a ship's propulsion system. Part I. Comparative investigation of calculated and measured torsional-axial vibrations in the shafting of a dry cargo motorship. C. A. M. van der Linden, H. H. 't Hart and E. R. Dolfin, 1968.
117 S A comparative study on four different passive roll damping tanks. Part II. J. H. Vugts, 1969.
118 M Stern gear arrangement and electric power generation in ships propelled by controllable pitch propellers. C. Kapsenberg, 1968.
119 M Marine diesel engine exhaust noise. Part IV. Transferdamping data of 40 modelvariants of a compound resonator silencer. J. Buiten, M. J. A. M. de Regt and W. P. Hanen, 1968.
120 C Durability tests with prefabrication primers in use steel of plates. A. M. van Londen and W. Mulder, 1970.
121 S Proposal for the testing of weld metal from the viewpoint of brittle fracture initiation. W. P. van den Blink and J. J. W. Nibbering, 1968.
122 M The corrosion behaviour of cunifer 10 alloys in seawaterpiping-systems on board ship. Part I. W. J. J. Goetzee and F. J. Kievits, 1968.
123 M Marine refrigeration engineering. Part III. Proposal for a specification of a marine refrigerating unit and test procedures. J. A. Knobbout and R. W. J. Kouffeld, 1968.
124 S The design of U-tanks for roll damping of ships. J. D. van den Bunt, 1969.
125 S A proposal on noise criteria for sea-going ships. J. Buiten, 1969.
126 S A proposal for standardized measurements and annoyance rating of simultaneous noise and vibration in ships. J. H. Janssen, 1969.
127 S The braking of large vessels II. H. E. Jaeger in collaboration with M. Jourdain, 1969.
128 M Guide for the calculation of heating capacity and heating coils for double bottom fuel oil tanks in dry cargo ships. D. J. van der Heeden, 1969.
129 M Residual fuel treatment on board ship. Part III. A. de Mooy, P. J. Brandenburg and G. G. van der Meulen, 1969.
130 M Marine diesel engine exhaust noise. Part V. Investigation of a double resonatorsilencer. J. Buiten, 1969.
131 S Model and full scale motions of a twin-hull vessel. M. F. van Sluijs, 1969.
132 M Torsional-axial vibrations of a ship's propulsion system. Part II. W. van Gent and S. Hylarides, 1969.
133 S A model study on the noise reduction effect of damping layers aboard ships. F. H. van Tol, 1970.
134 M The corrosion behaviour of cunifer-10 alloys in seawaterpiping-systems on board ship. Part II. P. J. Berg and R. G. de Lange. 1969.
135 S Boundary layer control on a ship's rudder. J. H. G. Verhagen, 1970.
136 S Observations on waves and ship's behaviour made on board of Dutch ships. M. F. van Sluijs and J. J. Stijnman, 1971.
137 M Torsional-axial vibrations of a ship's propulsion system. Part III. C. A. M. van der Linden, 1969.
138 S The manoeuvrability of ships at low speed. J. P. Hooft and M. W. C. Oosterveld, 1970.
139 S Prevention of noise and vibration annoyance aboard a sea-going passenger and carferry equipped with diesel engines. Part I. Line of thoughts and predictions. J. Buiten, J. H. Janssen, H. F. Steenhoek and L. A. S. Hageman, 1971.
140 S Prevention of noise and vibration annoyance aboard a sea-going passenger and carferry equipped with diesel engines. Part II. Measures applied and comparison of computed values with measurements. J. Buiten, 1971.
141 S Resistance and propulsion of a high-speed single-screw cargo liner design. J. J. Muntjewerf, 1970.
142 S Optimal meteorological ship routeing. C. de Wit, 1970.
143 S Hull vibrations of the cargo-liner "Koudekerk". H. H. 't Hart, 1970.
144 S Critical consideration of present hull vibration analysis. S. Hylarides, 1970.
145 S Computation of the hydrodynamic coefficients of oscillating cylinders. B. de Jong, 1973.
146 M Marine refrigeration engineering. Part IV. A Comparative stuyd on single and two stage compression. A. H. van der Tak, 1970.
147 M Fire detection in machinery spaces. P. J. Brandenburg, 1971.
148 S A reduced method for the calculation of the shear stiffness of a ship hull. W. van Horssen, 1971.
149 M Maritime transportation of containerized cargo. Part II. Experimental investigation concerning the carriage of green coffee from Colombia to Europe in sealed containers. J. A. Knobbout, 1971.
150 S The hydrodynamic forces and ship motions in oblique waves. J. H. Vugts, 1971.

151 M Maritime transportation of containerized cargo. Part I. Theoretical and experimental evaluation of the condensation risk when transporting containers loaded with tins in cardboard boxes. J. A. Knobbout, 1971.
152 S Acoustical investigations of asphaltic floating floors applied on a steel deck. J. Buiten, 1971.
153 S Ship vibration analysis by finite element technique. Part II. Vibration analysis. S. Hylarides, 1971.
155 M Marine diesel engine exhaust noise. Part VI. Model experiments on the influence of the shape of funnel and superstructure on the radiated exhaust sound. J. Buiten and M. J. A. M. de Regt, 1971.
156 S The behaviour of a five-column floating drilling unit in waves. J. P. Hooft, 1971.
157 S Computer programs for the design and analysis of general cargo ships. J. Holtrop, 1971.
158 S Prediction of ship manoeuvrability. G. van Leeuwen and J. M. J. Journée, 1972.
159 S DASH computer program for Dynamic Analysis of Ship Hulls. S. Hylarides, 1971.
160 M Marine refrigeration engineering. Part VII. Predicting the control properties of water valves in marine refrigerating installations A. H. van der Tak, 1971.
161 S Full-scale measurements of stresses in the bulkcarrier m.v. 'Ossendrecht'. 1st Progress Report: General introduction and information. Verification of the gaussian law for stress-response to waves. F. X. P. Soejadi, 1971.
162 S Motions and mooring forces of twin-hulled ship configurations. M. F. van Sluijs, 1971.
163 S Performance and propeller load fluctuations of a ship in waves. M. F. van Sluijs, 1972.
164 S The efficiency of rope sheaves. F. L. Noordegraaf and C. Spaans, 1972.
165 S Stress-analysis of a plane bulkhead subjected to a lateral load. P. Meijers, 1972.
166 M Contrarotating propeller propulsion, Part I, Stern gear, line shaft system and engine room arrangement for driving contrarotating propellers. A. de Vos, 1972.
167 M Contrarotating propeller propulsion. Part II. Theory of the dynamic behaviour of a line shaft system for driving contrarotating propellers. A. W. van Beek, 1972.
169 S Analysis of the resistance increase in waves of a fast cargo ship. J. Gerritsma and W. Beukelman, 1972.
170 S Simulation of the steering- and manoeuvring characteristics of a second generation container ship. G. M. A. Brummer, C. B. van de Voorde, W. R. van Wijk and C. C. Glansdorp, 1972.
172 M Reliability analysis of piston rings of slow speed two-stroke marine diesel engines from field data. P. J. Brandenburg, 1972.
173 S Wave load measurements on a model of a large container ship. Tan Seng Gie, 1972.
174 M Guide for the calculation of heating capacity and heating coils for deep tanks. D. J. van der Heeden and A. D. Koppenol, 1972.
175 S Some aspects of ship motions in irregular beam and following waves. B. de Jong. 1973.
176 S Bow flare induced springing. F. F. van Gunsteren, 1973.
177 M Maritime transportation of containerized cargo. Part III. Fire tests in closed containers. H. J. Souer, 1973.
178 S Fracture mechanics and fracture control for ships. J. J. W. Nibbering, 1973.
179 S Effect of forward draught variation on performance of full ships. M. F. van Sluijs and C. Flokstra, 1973.
182 S Finite element analysis of a third generation containership. A. W. van Beek, 1973.
183 M Marine diesel engine exhaust noise. Part VII. Calculation of the acoustical performance of diesel engine exhaust systems. J. Buiten, E. Gerretsen and J. C. Vellekoop, 1974.
184 S Numerical and experimental vibration analysis of a deckhouse. P. Meijers, W. ten Cate, L. J. Wevers and J. H. Vink, 1973.
185 S Full scale measurements and predicted seakeeping performance of the containership "Atlantic Crown". W. Beukelman and M. Buitenhek, 1973.
186 S Waves induced motions and drift forces on a floating structure. R. Wahab, 1973.
187 M Economical and technical aspects of shipboard reliquefaction of cargo "Boil-off" for LNG carriers. J. A. Knobbout, 1974.
188 S The behaviour of a ship in head waves at restricted water depths. J. P. Hooft, 1974
189 M Marine diesel engine exhaust noise. Part VIII. A revised mathematical model for calculating the acoustical source strength of the combination diesel engine – exhaust turbine. P. J. Brandenburg, 1974.
190 M Condition monitoring, trend analysis and maintenance prediction for ship's machinery (literature survey). W. de Jong, 1974.
192 S Hull resonance no explanation of excessive vibrations. S. Hylarides, 1974.
194 M On the potentialities of polyphenylene oxide (PPO) as a wet-insulation material for cargo tanks of LNG-carriers. G. Opschoor, 1974.

Communications

15 M Refrigerated containerized transport (Dutch). J. A. Knobbout, 1967.
16 S Measures to prevent sound and vibration annoyance aboard a seagoing passenger and carferry, fitted out with dieselengines (Dutch). J. Buiten, J. H. Janssen, H. F. Steenhoek and L. A. S. Hageman, 1968.
17 S Guide for the specification, testing and inspection of glass reinforced polyester structures in shipbuilding (Dutch). G. Hamm, 1968.
18 S An experimental simulator for the manoeuvring of surface ships. J. B. van den Brug and W. A. Wagenaar, 1969.
19 S The computer programmes system and the NALS language for numerical control for shipbuilding. H. le Grand, 1969.
20 S A case study on networkplanning in shipbuilding (Dutch). J. S. Folkers, H. J. de Ruiter, A. W. Ruys, 1970.
21 S The effect of a contracted time-scale on the learning ability for manoeuvring of large ships (Dutch). C. L. Truijens, W. A. Wagenaar, W. R. van Wijk, 1970.
22 M An improved stern gear arrangement. C. Kapsenberg, 1970.
23 M Marine refrigeration engineering. Part V (Dutch). A. H. van der Tak, 1970.
24 M Marine refrigeration engineering. Part VI (Dutch). P. J. G. Goris and A. H. van der Tak, 1970.
25 S A second case study on the application of networks for productionplanning in shipbuilding (Dutch). H. J. de Ruiter, H. Aartsen, W. G. Stapper and W. F. V. Vrisou van Eck, 1971.
26 S On optimum propellers with a duct of finite length. Part II. C. A. Slijper and J. A. Sparenberg, 1971.
27 S Finite element and experimental stress analysis of models of shipdecks, provided with large openings (Dutch). A. W. van Beek and J. Stapel, 1972.
28 S Auxiliary equipment as a compensation for the effect of course instability on the performance of helmsmen. W. A. Wagenaar, P. J. Paymans, G. M. A. Brummer, W. R. van Wijk and C. C. Glansdorp, 1972.
29 S The equilibrium drift and rudder angles of a hopper dredger with a single suction pipe. C. B. van de Voorde, 1972.
30 S A third case study on the application of networks for productionplanning in shipbuilding (Dutch). H. J. de Ruiter and C. F. Heijnen, 1973.
31 S Some experiments on one-side welding with various backing materials. Part I. Manual metal arc welding with coated electrodes and semi-automatic gas shielded arc welding (Dutch). J. M. Vink, 1973.
32 S The application of computers aboard ships. Review of the state of the art and possible future developments (Dutch). G. J. Hogewind and R. Wahab, 1973.
33 S FRODO, a computerprogram for resource allocation in networkplanning (Dutch). H. E. I. Bodewes, 1973.
34 S Bridge design on dutch merchant vessels; an ergonomic study. Part I: A summary of ergonomic points of view (Dutch). A. Lazet, H. Schuffel, J. Moraal, H. J. Leebeek and H. van Dam, 1973.
35 S Bridge design on dutch merchant vessels; an ergonomic study. Part II: First results of a questionnaire completed by captains, navigating officers and pilots. J. Moraal, H. Schuffel and A. Lazet, 1973.
36 S Bridge design on dutch merchant vessels; an ergonomic study. Part III: Observations and preliminary recommendations. A. Lazet, H. Schuffel, J. Moraal, H. J. Leebeek and H. van Dam, 1973.
37 S Application of finite element method for the detailed analysis of hatch corner stresses (Dutch), J. H. Vink, 1973.